



NAZARBAYEV
UNIVERSITY

**The serum dependent transcriptomic and gene expression analysis in
KRAS mutant cancer cells**

NARGIZ RAKHIMGEREY

(B.Sc. in Engineering and Technology, Y.A. Buketov Karaganda State University)

A THESIS SUBMITTED IN PARTIAL FULFILLMENT OF THE
REQUIREMENT OF NAZARBAYEV UNIVERSITY FOR THE
DEGREE OF MASTER OF SCIENCE IN BIOLOGICAL SCIENCES
AND TECHNOLOGIES

APRIL 2023

Student:	Nargiz Rakhimgerey	03/04/2023
Supervisor(s):	Professor Dos Sarbasov	03/04/2023

Examiners

The M.Sc. thesis of Nargiz Rakhimgerey has been approved by the examiners.

Associate Professor Tursonjan Tokay (School of Sciences and Humanities,
Department of Biology)

Professor Nikolai Barlev (School of Medicine, Department of Biomedical Sciences)

© April 2023

Nargiz Rakhingerey

All Rights Reserved

Declaration

I declare that the research contained in this thesis, unless otherwise formally indicated within the text, is my original work. The thesis has been written by me its entirety. I duly acknowledged all sources of information which have been used in the thesis. The thesis has not been previously submitted to this or any other university for a degree and does not incorporate any material already submitted for a degree.

Nargiz Rakhimgerey



03.04.2023

Acknowledgments

First and foremost, I would like to express my deepest gratefulness to my thesis supervisor, professor Dos Sarbassov, who accepted me despite my different research background to his research team. Thereby, I was given an opportunity to learn and contribute to the nutrient-dependent cell growth regulation studies. Under his supervision, Dr. Sarbassov taught me to think scientifically and shared opportunities to investigate the field of molecular oncology and biochemistry by providing an access to valuable knowledge and experience that he has. With his support, I feel that I am growing as a young researcher and finding my place in the world of modern biology.

Also, I would like to express my deepest appreciation to the Ministry of Education and Science for the opportunity to do my master's degree here and for awarding me with the scholarship to study.

Moreover, I am extremely grateful to Biology Department at Nazarbayev University for their invaluable knowledge and effort to expand my knowledge, the facilities that they provided and the supportive faculty that is always in the right place at the right moment.

I would like to extend my sincere thanks to Bayansulu Ilyassova, the Research Assistant in Dr. Sarbassov's laboratory. I could not have undertaken this journey without her, who taught me to all methods applied in this lab, and all the basic knowledge needed in any laboratory. Thank you for trusting and believing in me.

Of course, Many thanks to all my labmates, Aiman Jalmukhambetova, Aruzhan Dildabek, Dr. Agata Burska, Daurenbek Kairat and Askar Mazhikenov for their endless support, fruitful scientific discussions, love, and care that they shared with me. All of them were always by my side during my training and during these hard Master's thesis times. After coming to the lab, I found more than just colleagues, they become my second family who was always ready to help and support me, especially Aiman who was like a young sister to me, but her advice is always mature and senseful.

Many thanks to my NUZYP-mates, groupmates, and friends that I have found at Nazarbayev University, especially Zhazira Zhumabekova, who always shared her experience, and was so kind during my whole journey, listening to all my faults and disappointments, and being always nearby.

All gratitude should go to my mother and brother, for being with me throughout my life and creating conditions for me to go for my dreams. They were my mental and emotional support, we had a lot of calls full of care, support, and drama from my side. Thank you for your patience, love and for reminding me my goals. Their prayer for me was what sustained me this far.

I am grateful to everyone who has supported me throughout this process. Without your help and guidance, this thesis would not have been possible.

Table of Contents

Examiners	1
Declaration	3
Acknowledgments	4
Table of Contents	5
Abstract.....	7
List of Tables.....	9
List of Figures	10
Abbreviations	12
1 INTRODUCTION.....	13
1.1. Cancer and role of RAS protein mutations.....	13
1.2. Nutrient deprivation is a Hallmark of Cancer.....	14
1.3. Lipid biosynthesis and metabolic reprogramming in KRAS cancer cells.....	15
1.4. Serum-deprived conditions in cancer research	15
1.5. mTOR is the orchestrator of nutrient uptake	16
1.6. RNA is a key to understanding cancer phenotype.....	17
1.7. Aims & Hypothesis of the thesis project	18
2 MATERIALS AND METHODS	18
2.1 Cell culture	18
2.2 Methods and Instrumentation for Biochemical analysis.....	19
2.3 NGS sequencing and gene profiling	21
2.4 Primer designing	21
2.5 PCR analysis	22
2.5.1 Conventional PCR-based	22
2.5.2 RT-qPCR-based	22
2.6 Flow cytometry assay.....	22
2.7 Statistical analysis	23
3 Results	24
3.1. Cells under serum deprived conditions.....	24
3.2. Biochemistry analysis results.....	30
3.3. NGS sequencing and gene analysis results	32
3.4. Functional analysis.....	36

3.4.1	Conventional PCR based	36
3.4.2	RT-qPCR-based validation.....	37
4	Discussion	41
	Summary	42
6	Limitations	43
	Bibliography	44
	Supplemented materials	49

Abstract

Human cancers carrying KRAS mutations are considered to be highly malignant and are associated with poor prognosis, resistance to therapy, and highly adaptive to stress conditions. Nowadays, a growing body of literature indicates that a fetal bovine serum (FBS) supplement is a critical factor in cell culture medium providing growth factors and extracellular matrix components. Therefore, deprivation of this supplement is a common way to provoke stress associated with significant changes in cell growth and proliferation. The scientific community put huge effort to investigate cancer cell responses to serum deprivation and an explanation of its regulatory mechanisms. However, it is still unknown what happens with KRAS mutant cancer cells during serum deprivation. In this study, we investigated the changes of patterns ribosome/polysome profiling and transcriptomic gene expression in KRAS mutant cancer cell lines following serum deprivation. First, we studied the response of KRAS mutant cancer cells to serum deprivation by examining cell growth by cell number and cell size. Then, we performed the functional gene expression studies by performing transcriptomic analysis of the RNA obtained from total lysates and polysomal fraction. Using RNA sequencing analysis, we show that the genes involved in cholesterol and fatty acid synthesis are dramatically upregulated under serum starvation conditions in KRAS mutant cancer cells. The identified genes were further validated by the Q-PCR application. It is likely, we observe a main adaptive serum depletion response to compensate an abundance of cholesterol by activation of pathway responsible for its synthesis, because serum (FBS) is a main source of lipids including cholesterol in cell culture. A cellular pathway orchestrating this process is yet to be defined. The results of this study provide a better understanding of the molecular mechanism underlying the adaptation and survival of KRAS mutant cancer cells under serum deprived condition, understanding the biology of cancer cells behavior that in future may lead to development of novel therapeutic strategies for the treatment of KRAS mutant cancers.

Keywords: Kirsten rat sarcoma mutant cancer, cancer cells, RNP complexes, NGS, transcriptomic analysis, gene expression.

The serum dependent transcriptomic and gene expression analysis in KRAS mutant cancer cells

Nargiz Rakhingerey

List of Tables

Table 1. A quantitative representation of mRNA of FASN and ACAT2 genes associated with the polysomal fractions.....	33
Table 2. Representation of Cq values f FASN gene depends on a cDNA sample type	38
Table 3. Representation of Cq values of FASN gene depends on a cDNA sample type.	40
Table S1. Summary of research articles investigating serum deprivation conditions' effect on cancer cell line behavior.....	49
Table S2. Table Primers for identification of cholesterol pathway specific genes.....	51
Table S3. List of reagents	51

List of Figures

Figure 1. The representation of Ras effector pathways [7].	14
Figure 2. Schematic representation of cell culture condition.	19
Figure 3. Schematic representation of cell lysis, subcellular fractionation, RNP complexes separation.	20
Figure 4. A549 cell line images across three timelines 24, 48 and 72h. Left side is all images for cells grown in complete media, right side images of cells grown in FBS-deprived. (A) and (B) images for 24h, (C), (D) and (E), (F) for 48h and 72h, respectively.	25
Figure 5. Dot plots for the A549 cell line growth model under the FBS-deprived conditions point out cell number and cell size across the three time periods. (A) and (B) represents 24h, while (C), (D) and (E), (F) represent 48 and 72h, respectively, (ns; not significant, **; $P < 0.01$, ***; $P < 0.001$, Unpaired t-test).	26
Figure 6. PI-positive cell percentage of A549 cells by Flow Cytometry assay, (24hrs, ns; not significant, Unpaired t-test).	28
Figure 7. PI-positive cell percentage of HeLa cells by Flow Cytometry assay, (24hrs, **; $p < 0.01$, Unpaired t-test).	29
Figure 8. Flow cytometry results for A549 (A) and HeLa (B) cells at 48h in complete GM with FBS and without FBS. Cell death detected by PI staining positive cell percentage. (48hrs, ns; not significant, ***; $p < 0.001$, Unpaired t-test).	30
Figure 9. The ribosome/polysome profiling of A549 cancer cells incubated for 24h with serum (10% FBS) represented by blue line or without serum represented by the black line in the graph.	31
Figure 10. The ribosome/polysome profiling of HeLa cancer cells incubated for 24h with serum (10% FBS) represented by black line or without serum represented by the blue line in the graph.	32
Figure 11. The heatmap of transcriptomic analysis of polysomal and 80S fractions from serum deprived conditions and GM. All samples labeled with 0% on the bottom of X-axis are FBS deprived conditions, while Y-axis shows the genes that overexpressed.	35
Figure 12. Agarose gel electrophoresis for target genes FASN and ACAT2. (1) 18S rDNA Control conditions; (2) FASN control total; (3) FASN 0FBS total; (4) FASN control polysomal; (5) FASN 0FBS polysomal; (6) ACAT2 control total; (7) ACAT2 0FBS total; (8) ACAT2 control (control) polysomal; (9) ACAT2 0FBS polysomal.	37
Figure 13. Representation of qPCR amplification for FASN gene. Curves for the conditions are bold. (A) FASN amplification for control total RNA; (B) FASN amplification for FBS deprived total RNA; (C) nonspecific control cDNA.	38
Figure 14. Representation of qPCR amplification for ACAT2 gene. Curves for the conditions are bold. (A) ACAT2 amplification for control total RNA; (B) ACAT2 amplification for FBS deprived total RNA; (C) nonspecific control cDNA.	40

Figure S1. Dot plots for the HeLa cell line growth model under the FBS-deprived conditions point out cell number and cell size across the three time periods. (A) and (B) represents 24h, while (C), (D) represents 48h, (ns; not significant, **; P<0.01, ***; P<0.001, Unpaired t-test). 52

Figure S2. Dot plots for the A549 cell line growth model under the Complete medium (GM) and FBS-deprived (0%FBS) conditions point out cell size at 16hrs, (***) P<0.001, Unpaired t-test). 53

Figure S3. The ribosome/polysome profiling of A549 cancer cells incubated for 24h in media with glucose supplement represented by blue line or without glucose supplement represented by the black line in the graph. 54

Figure S4. The ribosome/polysome profiling of A549 cancer cells incubated for 24h with serum with complete media represented by blue line or without amino acid supplement represented by the black line in the graph. 55

Figure S5. The ribosome/polysome profiling of HEK293 cancer cells incubated for 24h with serum (10% FBS) represented by black line or without serum represented by the blue line in the graph. 56

Abbreviations

RAS	Rat sarcoma
KRAS	Kirsten rat sarcoma
ACAT2	acetyl-CoA acetyltransferase 2
FASN	Fatty acid synthase
GDP	Guanosine diphosphate
GTP	Guanosine triphosphate
mTOR	mammalian Target of Rapamycin
FBS	Fetal bovine serum
GFR	Growth Factor receptor
RNP	Ribo nucleoprotein
NGS	Next generation sequence
PCR	Polymerase chain reaction
RT-qPCR	Real-time quantitative polymerase chain reaction
PI3K	Phosphoinositide 3-kinase
PDAC	Pancreatic ductal adenocarcinoma
DMEM	Dulbecco's Modified Eagle Medium
PI	Propidium iodide
PCA	Principal component analysis
ICA	Independent component analysis

1 INTRODUCTION

In recent years, most of the literature considered dysregulation of cellular metabolism as the driver causative which helps cancer cells develop and survive during diverse circumstances, thereby making them resistant to the variety of treatments. Therefore, there is an urgent need to understand basic metabolic differences between cancer and primary (normal) cells. This study aimed to characterize deviations of transcriptomic data and gene expression of cancer cell lines depending on the absence of serum that is critical for cell growth and proliferation.

1.1. Cancer and role of RAS protein mutations

Cancer is a second worldwide problem of public health that caused the death of 1 in 6 people in 2018, which comprised about 9.6 million deaths, and these indicators continue to grow [1]. They also proposed, the reason for such a burden is the problems with treatments and predicting cancer development due to its complexity and variety of responses for different conditions. That is why cancer is considered a result of complex events. During the last decades, scientists consider that most of the difficulties of cancer cases are caused by RAS gene-specific mutation, which is the important oncogenic driver with 3 existing isoforms: N isoform (NRAS), K isoform (KRAS), and H isoform (HRAS). According to the literature [2], NRAS contains 17% of RAS-driven mutations, while HRAS composed only 7%. In contrast to this, K isoform RAS-type mutations are the most prevalent, with a frequency of about 20 mutations per 29 detected cancers among all types. This particular mutation is present almost 100% in Pancreatic ductal adenocarcinoma (PDAC), and also mostly in colon and lung cancer cells [3], [4]. The main function of the KRAS gene is to encode the KRAS protein, which switches from a guanosine diphosphate (GDP) inactive state by binding to guanosine triphosphate (GTP) to acquire a permanently active state [5]. Also, this active KRAS protein is the central part of the multiple cellular pathways since it couples cell membrane growth factors to signaling pathway mediators, like kinase residues, transcription factors, and pathway regulators themselves. As it has been reported in most of the papers [2], [6] when this gene is oncogenically activated there is a tight binding with the GTP molecule, which makes the KRAS protein constantly active and leads to uncontrollable cell growth and cell cycle damage by triggering various cellular pathways endlessly, like axes of PI3K-AKT-mTOR regulators of cell growth (Figure 1). Figure below shows in which intracellular pathways RAS is involved.

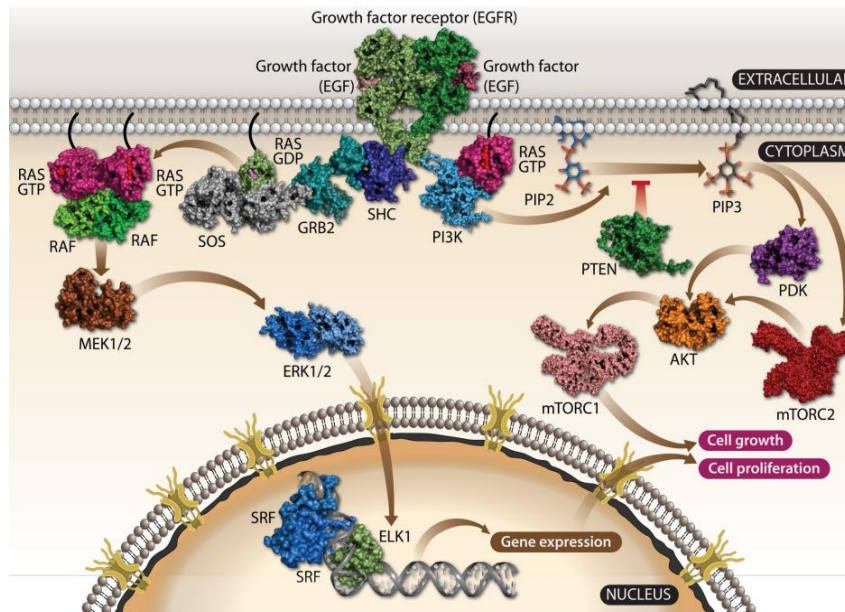


Figure 1. The representation of Ras effector pathways [7].

Also, these axes are considered a key effector of the oncogenesis driven by KRAS mutation. At the beginning of the previous decade, it was clearly characterized [8] that activation of this mTOR pathway is highly involved in the Warburg effect, which states that tumor cells to survive and complete cancerogenesis increase glucose uptake. This shows that any cancerogenesis is driven not only through the mutant-driven actions, but is something more complex and cyclic in accompanying metabolic processes and cellular pathway regulations.

1.2. Nutrient deprivation is a Hallmark of Cancer

According to some papers [9], [10] cancer is a multistep process that relies on various dysregulations, which are called “cancer hallmarks”. Authors [9] pointed out that one of the last hallmarks that were considered and discussed more in 2011 [10] was cellular metabolic dysregulation, which later became a key point interacting with other hallmarks and triggering cancer development. Metabolic cellular reprogramming helps to survive cancer cells by making possible adaptations to the environmental changes and corresponding to the levels of cancer development, like initiation, cell growth, invasion, and metastasis formation [11]. They argue that this process is triggered by nutrient availability, especially with the over-uptake by cancer cells. Usually, uncontrollably growing cells as a source of nutrients use glucose, amino acids, and lipids, which are imported to support membranes, express proteins, and nucleic acids, and generate the energy source of Adenosine triphosphate (ATP) [12]. As it was reported [13], in recent years there was a tremendous effort to investigate the regulation of over-uptake of glucose, amino acids, and lipids in KRAS mutant cancer cells. For example, as was shown by group of authors [14] and others previously, over-uptake

of glucose is common for KRAS-driven cancer cells, and moreover this mutation trigger pathways to regulate this glucose addiction, and in the case of deprivation, there could be other ways to compensate for these glucose deficiencies. This last research system tries to compensate for glucose absence by lysosomal nutrient excretion pathways, which act usually as a recycling center for cells, but in this case, cells return unneeded nutrients that should go through lysosomal pathways. Previous evidence also suggests [10], that nutrient starvation is a main cause of stress for cancer cells, which affect their viability but also could be the source to manage stress and quickly adapt to it by increasing cell number rates due to invisible but present molecular mechanisms.

1.3. Lipid biosynthesis and metabolic reprogramming in KRAS cancer cells

As it was mentioned in previous part, metabolic reprogramming is one of the important hallmarks of aggressive cancer progression. This is tightly connected with mutations, such as MYC, KRAS, which usually responsible for new metabolic properties that help to increase proliferation, growth, and resistance to various treatment strategies [15]. That is why usually it is called oncogene-induced metabolic reprogramming. According to the literature [16], last decades over activated de novo synthesis of lipids in KRAS cancer cells become the most questionable metabolic reprogramming in cancer. In last years, it was investigated that fatty acid synthesis and its overexpression associated with de novo lipogenesis, and could be potential target as a distinct treatment strategy [17]. However, there is another broad category of lipid biosynthesis regulator as a cholesterol pathway, which is also often reported as an upregulated one in KRAS cancer cells [18]. Usually, it is characterized by the overexpression of genes, such as ACAT2, which catalyze molecules of acetyl-CoA, or by HMG-CoA reductases, which affect downstream targets of cholesterol pathway [19]. Despite the fact that there is a lot of pathways, enzymes and regulators are involved in lipid biosynthesis, the most attractive for cancer investigation still fatty acid and cholesterol synthase pathways. In cell culture environment will be interesting to investigate this pattern, especially when it is known that source of lipid for cells in vitro is a serum supplement.

1.4. Serum-deprived conditions in cancer research

In recent years growing body of literature put more attention to the serum starvation of cancer cells in vitro by excluding the main supplement fetal bovine serum (FBS) in cell culture media as an impactful nutrient condition since it mimics nutrient deprivation of cancer cell in vivo [20]. This could be due to the fact that the effect of the product and its composition is still not well understood, and results of cell growth could vary depending on the manufacturer or the cell line characteristic. Nevertheless, due to its importance in vitro cell culture medium, it is an attractive target to investigate. According to some authors [21], a lot of studies consider serum deprivation, but there

are still unknown clear mechanisms of the impact of condition absence or presence on cell regulation, and this situation remains the same. Also, they designated that serum-deprived conditions could be considered cell growing either in an FBS-free medium or in partially reduced FBS. Based on the already existing literature, serum-deprived conditions affect cell proliferation and activity. Moreover, could regulate intracellular activities, and results varied between studies probably depending on the cell lines and condition specifications [22], [23], [24]. These mentioned results for serum-deprived conditions in various cell lines were gathered and presented in Table S1 of Appendices. In this table, some controversial results could be observed, for example, one paper [25] reported cell death in breast cancer lines, like MDA-MB-231, MDA-MB-468, and other types, while another one [26] argue that during serum deprivation these above-listed cell lines are able to resist, and moreover to increase their proliferation rates. Also, some of the literature reported cell death in different cell lines during serum deprivation, which leads to the reasonable idea that could it be tightly connected to the KRAS mutation as in the case of nutrient-deprived conditions with glucose, and amino acids mentioned earlier. But in the case of both papers [25] [26], it little bit controversial, but still could be the reason since the author did not mention and focused specifically on the mutation type of the lines, however, usually, these breast cancer cell lines are considered to be KRAS-mutated [27]. So, all the literature in that table provides different consequences of serum deprivation and causes of resistance to the absence of serum, which mostly triggers various cellular pathways, which will be the key to understanding the common mechanism of nutrient uptake regulation.

1.5. mTOR is the orchestrator of nutrient uptake

As a continuation of the last part, organization, and regulation of this nutrient uptake at an appropriate time from the microenvironment without side effects should be done by a precise mechanism. According to the growing body of literature [28], the Mammalian target of Rapamycin (mTOR) is considered to be the orchestrator of all cellular reprogramming processes, since complexes of mTOR, like mTORC1 and mTORC2, not only involved in work of Growth factor receptor signalling (GFR), but also in RNP complexes formation, that will response to information about the availability of nutrients in the surrounding environment. Another group of authors [29] argue that mTOR-mediated nutrient dependence leads to changes in the RNP complex's biogenesis, which will affect the protein and gene expression of the cells. This also regulates the accumulation of cell growth and its mass. If there is nutrient uptake going on, this means that mTOR pathways are hyperactivated, which together also over-activate RNA polymerase 1 activity, which is a key player in ribosomal biogenesis [30]. This conclusion implies that high rates of nutrient uptake through mTOR signalling pathways are tightly connected with genomic modifications that include protein

expression, mRNA synthesis, and DNA instability.

1.6. RNA is a key to understanding cancer phenotype

Literature of this decade [31], [32], in order to investigate cellular modifications, give preference to RNA molecules, overall called transcriptome, rather than metabolome analysis, which is hard to obtain and analyze. Moreover, metabolites depend on the plentiful presence of enzymes, which are translated from mRNA [33]. According to them, these two pillars, metabolome, and transcriptome are highly intertwined through the reflection of changes in genotype and phenotype, which gives the opportunity to provide clear evidence about gene modifications, protein, and metabolite expression along with cellular mechanisms. Consequently, this raises questions as to whether it is possible to predict metabolic reactions and cancer growth through transcriptomic analysis since it is the most economically and scientifically efficient way to investigate the connection between the hallmarks discussed above. Moreover, RNA investigation is a better research approach than DNA in the case of cancer, because RNA gives more dynamic, non-identical sequences, which will reflect the phenotypes as a signature of cell states, and will give ideas about the uniqueness of each cell depending on various nutrient supply chains [34]. Authors also claim that transcriptomics is a powerful tool of gene profiling, which not only provides information about gene expression but also is able to generate data of modification, and structural changes across all cells along with pairwise comparisons of different gene expressions according to the various conditions implemented to the cells. Such an example was provided in recent paper [35], where they implemented folic acid deprivation conditions for breast cancer and did transcriptomic profiling with comparisons in gene expression during the presence and absence of folic acid. They identified that such deprivation conditions changed gene expression, especially on key breast cancer points, like interferon signaling genes and mesenchymal phenotype-responsible genes, which already gives an idea of which direction treatment strategies should be developed, and show distinct axes of treatment pathways that should be implemented.

In this research, the transcriptomic data will be essential since the classical way of ribosomal profiling will be an essential part to understand the molecular and biochemical properties of the cells under such serum-deprived conditions. That is why RNA isolation will be the key to this fundamental research that will show us the alterations in the gene expression level of cancer cell lines under serum-deprived conditions based on transcriptomic data analysis.

1.7. Aims & Hypothesis of the thesis project

Considering the information discussed above, this study is pursuing to investigate how KRAS mutant cancer cells response serum deprivation. The **hypothesis** of this thesis project is that serum deprivation of cancer cells turns on expression of particular mRNAs by their active translation in polysomes, which are responsible for cell survival and growth under serum deprivation of KRAS mutant cancer cell mediated by distinct signaling systems.

In order to test our hypothesis, we set the following aims:

- 1) To examine cell number and size of KRAS mutant cancer cells incubated in the cell culture medium with or without 10% fetal calf serum for 24 hours.
- 2) To perform isolation of the polysomes by a subcellular fractionation and sucrose gradient fractionation of KRAS mutant cancer cells incubated with or without 10% fetal calf serum.
- 3) To define the critical genes upregulated in response to serum deprivation of KRAS mutant cancer cell.

2 MATERIALS AND METHODS

Methods that will be used in this study were chosen according to the specificity of the aims mentioned in the previous part and experimental procedure.

2.1 Cell culture

The first and foremost part of this experiment is the cell culture and conditions that settled for this study. This part of the study compared cells based on their count, size, and morphology under two different conditions. 2 cell lines were used in this experiment: A549 – human KRAS mutant lung adenocarcinoma cell line. Cells were taken from laboratory stocks, which were initially obtained from American Type Culture Collection (ATCC, Rockville, MD, USA). All culture experiments were performed with cells not contaminated with mycoplasma. According to the cell culture protocols, these cell lines was maintained in Dulbecco's modified Eagle's medium F-12 (DMEM/F-12, US biological Life sciences, Way Salem, USA), supplemented with 10% fetal bovine serum (F7524, FBS, non-US origin, Sigma-Aldrich), Streptomycin sulfate salt (S9137-100G) and Penicillin G sodium salt (P3032) both ordered from Sigma Aldrich. Cells were cultured at 37°C in a humid incubator with 5% CO₂, which also controls high humidity. To investigate the effect of serum derived condition on KRAS cancer cells, FBS supplement was deleted from DMEM in which cells were maintained (Figure 2).

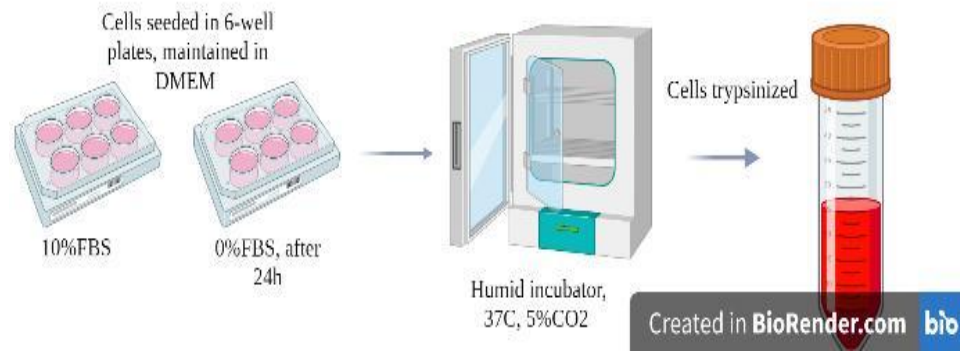


Figure 2. Schematic representation of cell culture condition.

Cells were seeded day prior transitioning them into DMEM/F-12 without FBS, in order to mimic serum-deprived conditions. Cell number and size were measured by Multisizer Coulter Counter 4e (B43905, Beckman Coulter, Life Sciences). To achieve that, cells were trypsinized, using diluted Trypsin (X0930-100, Biowest, Nuaille, France), an enzyme, which dissociates adherent cells from the plate, then suspension of cells will be placed to Multisizer, which works based on Electrical Sensing Zone principles, which is based on reading voltage pulses of suspended cells when they pass through an aperture, under an electrical current, and amplitude of this pulse is given the volume of the cells. The cell morphology was observed through ZEISS Primovert Inverted Microscope (Zeiss, Oberkochen, Germany). When condition settled for further work, cells were seeded to 150 mm big plates, using the same protocol adjusted for big plates since next biochemistry studies require high protein volumes.

2.2 Methods and Instrumentation for Biochemical analysis

Cell culture was followed by fundamental biochemical investigations that based on cell lysis, subcellular fractionation in order to obtain polysome fractions in ribosomal profiling (Figure 3).

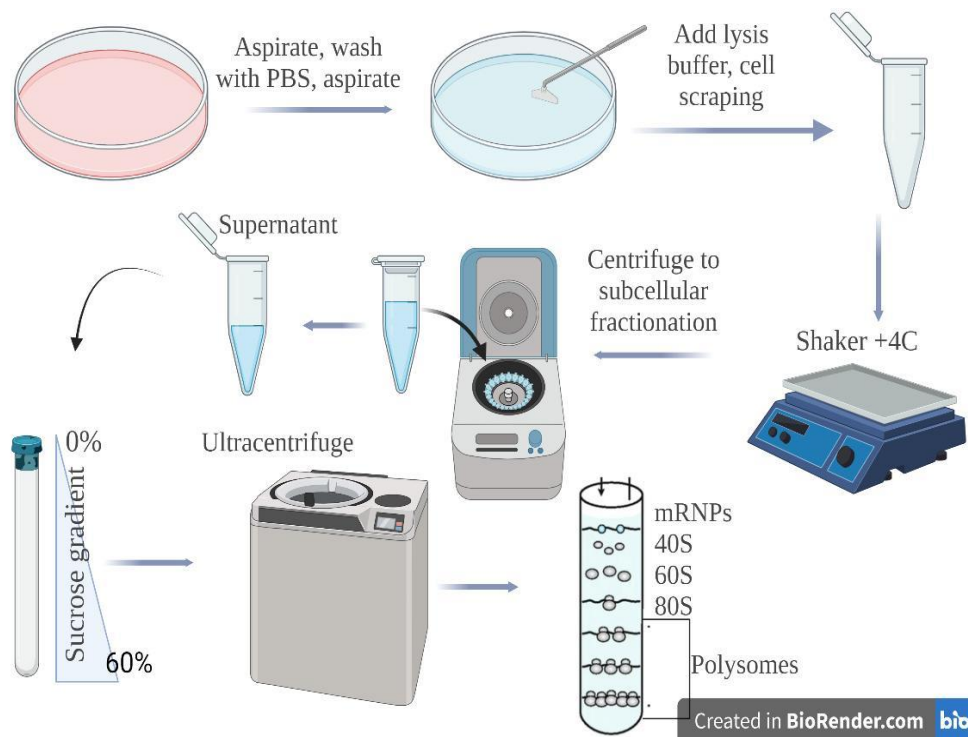


Figure 3. Schematic representation of cell lysis, subcellular fractionation, RNP complexes separation.

To achieve this, procedure starts from cell lysis with the specific cell lysis buffer – “Magnesium buffer with detergent”, which also contain protease inhibitor cocktail, which protects proteins from degradation. Lysis itself lasts for 30 min, at +4°C. Then subcellular fractionation starts. For this purpose, cells were centrifuged, and cytoplasm fraction was obtained. After that, cytoplasm lysates were fractionated by a linear sucrose gradient and ultracentrifugation to isolate the RNP complexes fractions, especially the polysomes. The BioComp Gradient Station with Triax flow cell 1 (Fredericton, Canada) was used as an instrument to obtain the highly reproducible linear sucrose gradients and perform the automated fractionation analysis. This tool is composed of a gradient station itself, a Gilson fraction collector, and a Triax flow cell, which gives the opportunity to record UV and fluorescence scans. As it is defined in the protocol, obtained lysates from previous step were loaded on top of the sucrose gradient. The gradient station creates the sucrose gradient through the patented process, which is called “tilted tube rotation”, controlled by 11-step gradient-making program. Before exploitation, gradient stored in the refrigerator (+4°C) to make them more viscous. The prepared lysates were placed on top of the gradients and fractionated by ultracentrifugation in a ThermoScientific Sorvall WX Ultra Series Centrifuge with ThermoScientific Sorvall Rotor Swinging bucket rotor TH-641. The sucrose gradients with lysates were profiled after fractionation by the BioComp gradient station with Triax flow cell 1 for monitoring UV light (254-nm wavelength) absorbance, obtaining about 24 to 28 fractions, where it was able to observe the 80S, 40S, and

polysomes. All fractions were collected into separate tubes. Detected RNP complexes from these fractions was isolated through PEG precipitation. Precipitated RNP complexes was used to isolate RNA with Trizol reagent (Thermo Fisher Scientific, USA) according to the manufacturer's instructions. RNA concentration and purity were measured by Nanodrop spectrophotometer (Thermo Fisher Scientific, USA). Obtained fractions and RNAs were stored at -20°C in Eppendorf tubes.

2.3 NGS sequencing and gene profiling

RNA isolation was followed by the quantification of RNA concentration through the fluorometric method Qubit RNA HS Assay Kit (Q32852, Invitrogen, USA). Then, there was RNA-seq library preparation using the Illumina TruSeq Stranded Total RNA kit and NEXTFLEX Small RNA-Seq Kit. Products was collected and sequenced using an Illumina HiSeq 2000. Obtained transcriptomic data was analyzed by the NLA bioinformatics lab [36] using STAR methodology, where differentially expressed genes was calculated through the DESeq pipeline. Also, validation of gene lists by enrichment analysis and pathway analysis was done through the KEGG Database, while sample analysis and data dimensionality reduction were performed by Principal Component Analysis. Moreover, additional analysis was done by ICA. After that, identified “essential” genes was processed through Rstudio programming language for statistical computing and graphs, where there were gene profiles, and gene ontology in a representative manner to characterize already identified genes.

2.4 Primer designing

Specific primers were prepared for the identified overexpressed genes. NCBI “Primer-Blast” was used as a primer designing tool. First, through the NCBI home page gene search was performed for each identified gene in order to obtain the right DNA template. To do that NCBI refseq accession number was used. When gene sequence and exon/intron parts are decided, procedure moved to Primer-Blast window, where forward and reverse primers range, melting temperature, also product size, and settings to avoid potential bindings and genomic contamination were chosen. When all is set, primer pairs were obtained and sent to synthesizing (Sigma Aldrich, USA). Primer’s sequences are listed in Table 2S.

2.5 PCR analysis

2.5.1 Conventional PCR-based

Designed primers based on NGS analysis are targeting the Fatty acid and cholesterol synthesizing genes. To validate these genes PCR was done according to the NEB protocol (M0273), using 2.5 μ M 10x Standard *Taq* reaction buffer, 0.5 μ M dNTPs (10mM), 1 μ L of each primer (10 μ M), 1 μ L template DNA, 0.125 μ L *Taq* DNA polymerase, and increased with nuclease free water until 25 μ L of reaction volume. When PCR mix is ready, samples were transferred to Thermocycler (Bio-Rad, California, USA). Thermocycling conditions were set according to the NEB protocol as following: initial denaturation for 30s at 95 $^{\circ}$ C, followed by 30 cycles of 30s at 95 $^{\circ}$ C, and 45s at 52 $^{\circ}$ C temperature based on a melting temperature calculation, and 1 min at 68 $^{\circ}$ C. The final extension step was last 5 min at 68 $^{\circ}$ C. Obtained PCR products were analyzed with gel electrophoresis, using 1.5% agarose gel, stained with Ethidium Bromide Solution (1610433, Bio-Rad, California, USA). Images were obtained through ChemiDoc MP Imaging System (Bio-Rad, California, USA).

2.5.2 RT-qPCR-based

The real-time quantitative PCR (qPCR) assay' first step was performed using the TaqMan Reverse Transcription Reagents (Applied Biosystems) according to the protocol. Then with the prepared cDNA, second step started by using SYBR Green PCR Master Mix (Applied Biosystems) according to the manufacturer protocol. Amplifications were carried out in 20 μ L reaction solutions containing 710 μ L 2x SYBR Green Master Mix (Applied Biosystems), 5 μ L first-stranded cDNA (1-100ng), 1.5 μ L of each specific primer with the working concentration 10 μ M, and 2 μ L nuclease-free water (Invitrogen). PCR conditions were 95 $^{\circ}$ C for 10 min polymerase activation followed by 40 cycles of 95 $^{\circ}$ C for 15 s and 60 $^{\circ}$ C for 1 min. The specificity of each pair of primers was checked by melting curve analysis. Further, make results statistically precise, each assay will be performed with technical triplicates.

2.6 Flow cytometry assay

Flow cytometry assay with Propidium iodide (PI) staining was used to analyze the dead cell population using Attune NxT acoustic focusing cytometry (Thermo Fisher Scientific, USA) equipped with blue laser emission rate 450nm. To prepare single cell suspension, cells were trypsinized, washed with 1X PBS, and diluted into Eppendorf tubes 300k cells per 500ul suspension in 1X PBS.

Stained with working solution of PI in ratio of 1:100. Incubated in the dark at room temperature for 15 min. Gating strategies were used to exclude debris and doublets. Recorded results were statistically analyzed using Graph Pad Prism 8.

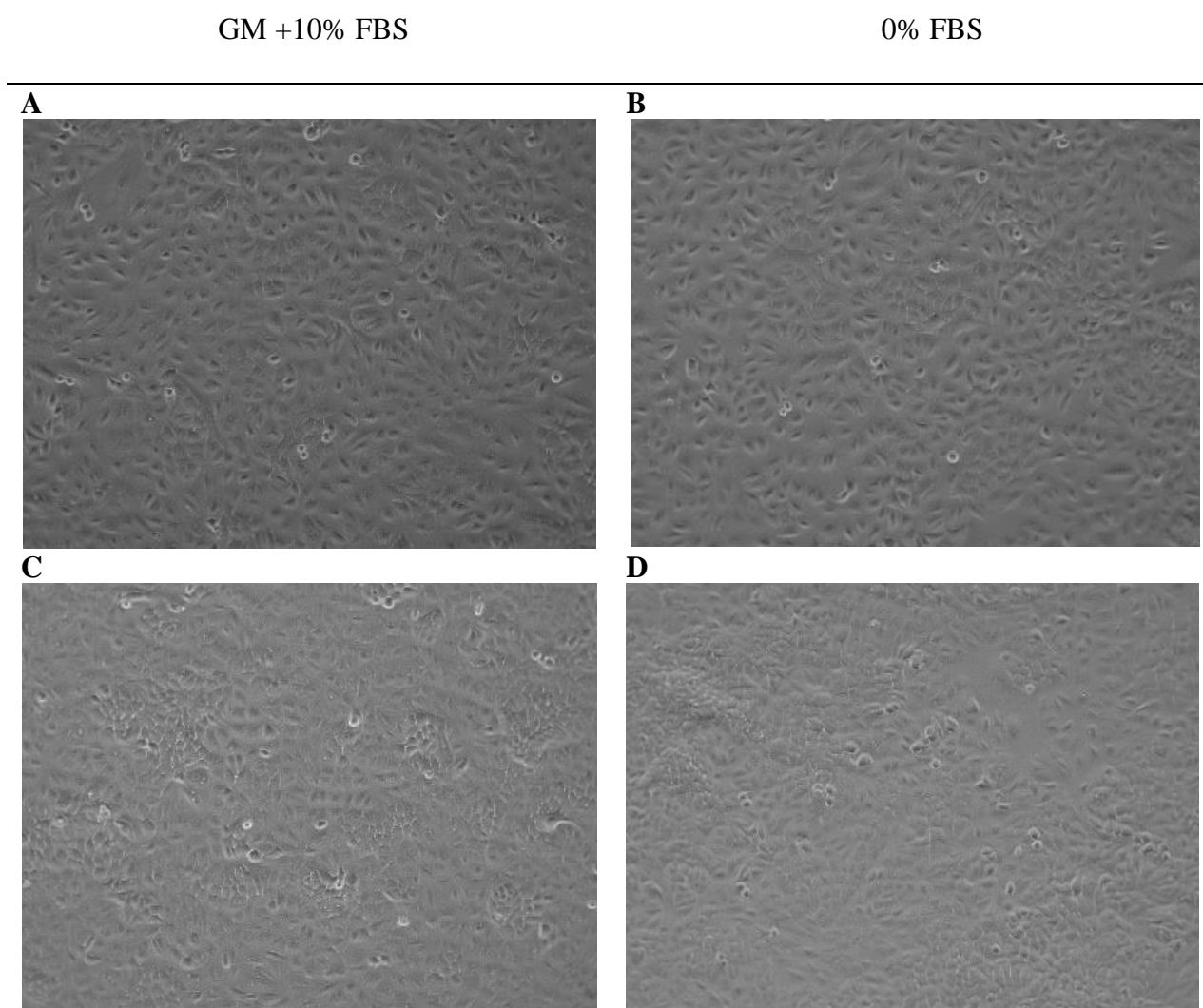
2.7 Statistical analysis

All statistical analyses and calculations were performed by Microsoft Excel 2019 (Microsoft, Washington, USA). GraphPad Prism 8 (San Diego, California, USA).

3 Results

3.1. Cells under serum deprived conditions

Despite the main aim of the thesis, which lies more on fundamental biochemistry investigations of cells under the stressed condition, we performed the functional transcriptomic study in A549 human cancer cells (the human lung cancer cell line) incubated in cell culture medium with or without 10% serum. Cells were cultured in growth media (GM) containing 10% FBS or 0% FBS (FBS-deprived) medium for 24, 48 or 72h in order to study the effects of serum deprivation. The cell images were taken prior making any analysis (Figure 4).



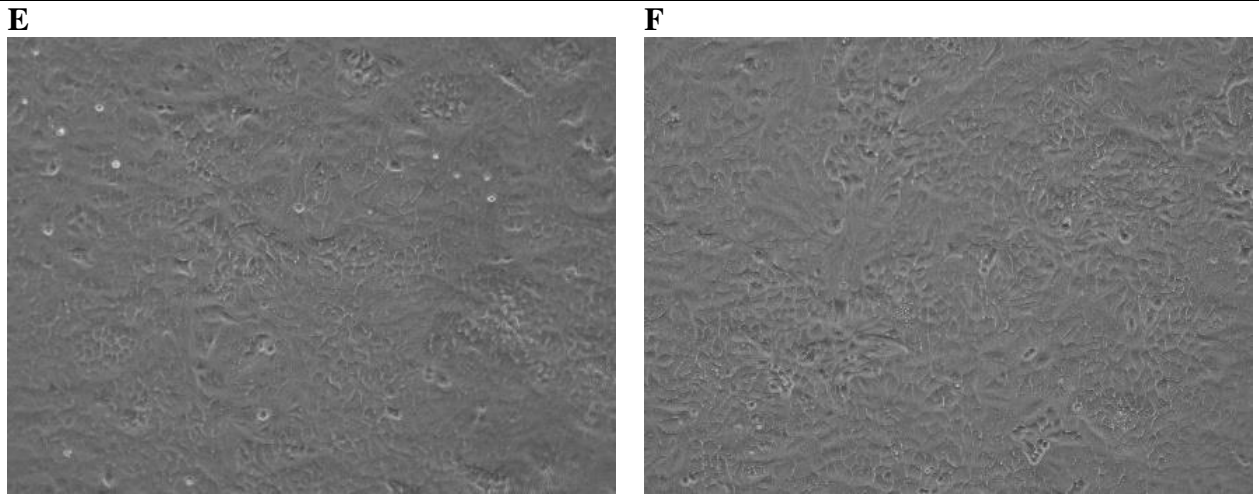
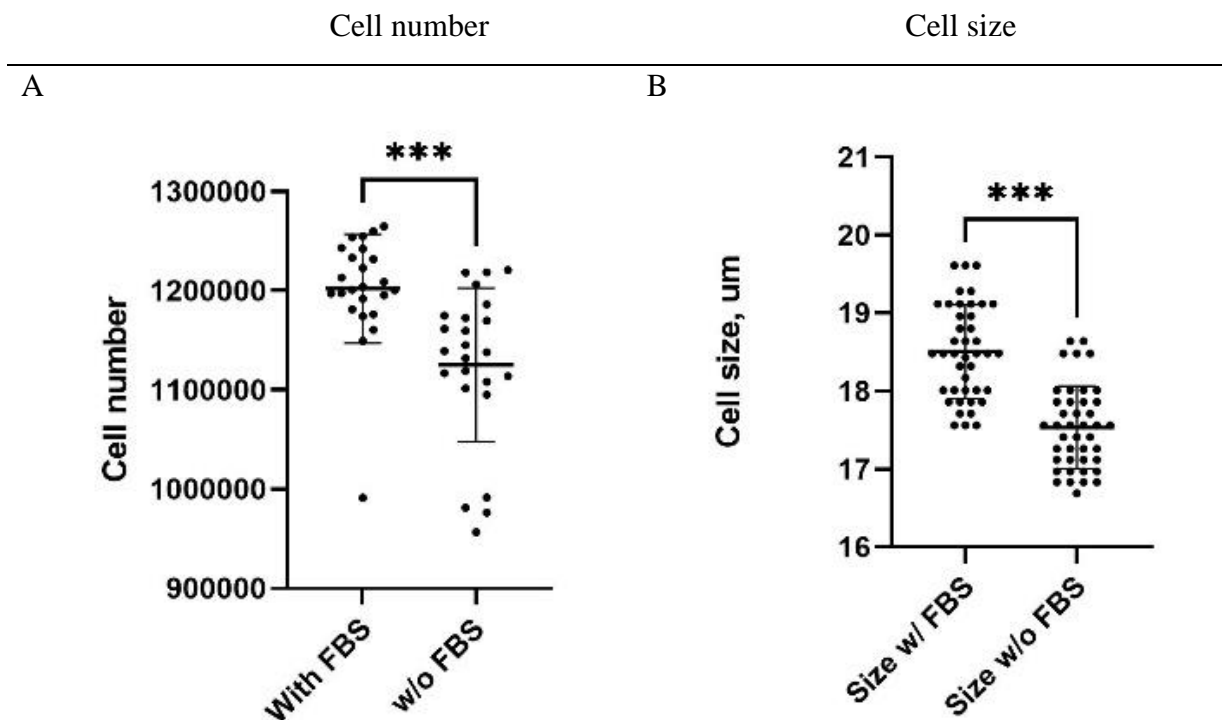


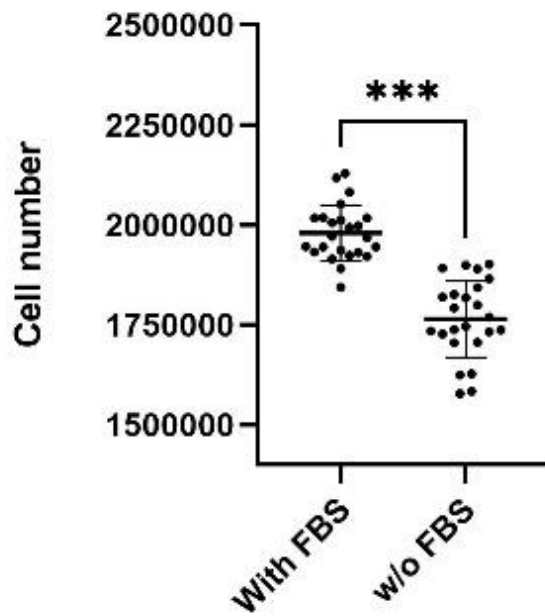
Figure 4. A549 cell line images across three timelines 24, 48 and 72h. Left side is all images for cells grown in complete media, right side images of cells grown in FBS-deprived. (A) and (B) images for 24h, (C), (D) and (E), (F) for 48h and 72h, respectively.

According to the Figure 4, it is visible that a cell density has increased over time. However, there is no distinct difference between the conditions as indicated by cell imaging, which needs validation by numbers to access the quantitative growth rate difference under this condition.

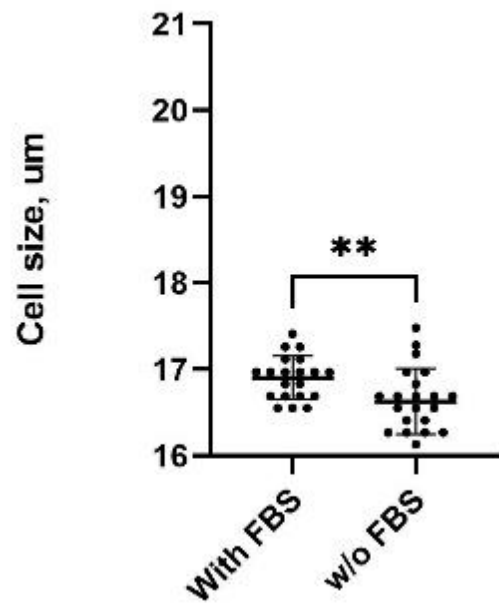
Serum deprivation showed statistically significantly difference in cell number, cell size in comparison with the A549 cells grown in DMEM/F-12 supplemented with FBS and without for 24h (Figure 5A, 5B).



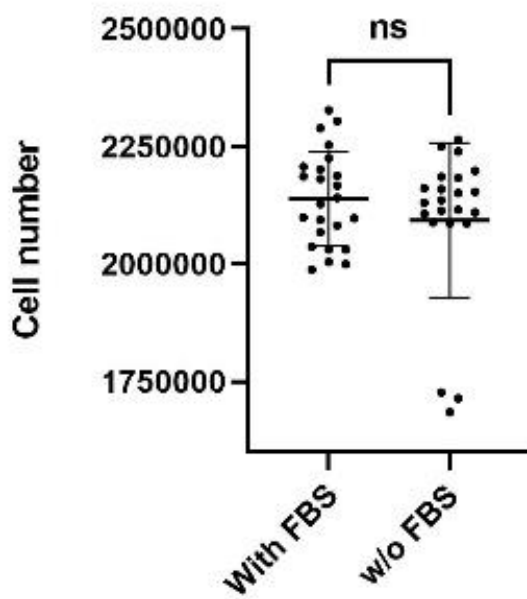
C



D



E



F

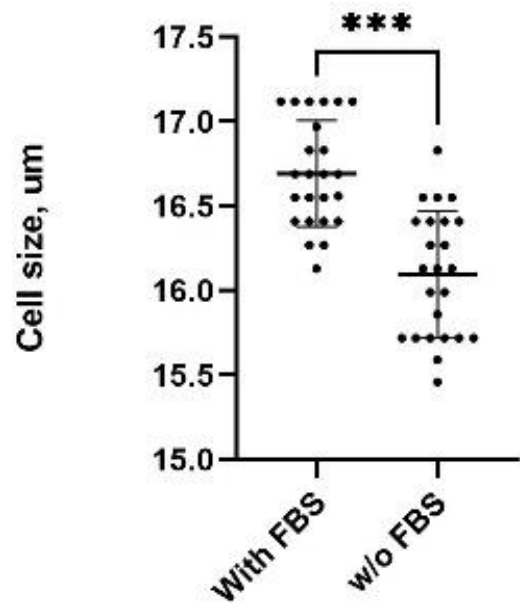


Figure 5. Dot plots for the A549 cell line growth model under the FBS-deprived conditions point out cell number and cell size across the three time periods. (A) and (B) represents 24h, while (C), (D) and (E), (F) represent 48 and 72h, respectively, (ns; not significant, **; $P < 0.01$, ***; $P < 0.001$, Unpaired t-test).

The same pattern from cells was observed following 48 hrs of incubation, but with less significance in cell size difference, which could be explained by a high confluency reached by cells in GM with FBS because a high growth rate affecting the cell size (Figure 5C, 5D). Moreover, this was approved by cell number observed in 72h (Figure 5E), since cells in GM that reached high density displayed less growth rate due to the nutrient exhaustion that caused a metabolic stress. Therefore, the difference in cell number between GM-grown and FBS-deprived cells is not significant. However, we observed a noticeable difference in cell size at the 72h of incubation (Figure 5F), where cell size decreased for 1um under serum deprived condition in comparison with 48h, where difference was equal for 0.3um. According to this data, we show that serum promotes cell growth. As represented in the last dot plot (Figure 5F), the serum also determines cell size and its absence is stressful for A549 KRAS cancer cells. However, for non-KRAS HeLa cells the difference in cell size between two groups was not significant at 24h and 48h time points, while cell number changes were significant the same as for A549 cancer cells (Figure S1). An observed serum-dependent effect on cell size in A549 cells starts at 16h (Figure S2) and continues for 72h.

The extension of time beyond 72h is problematic because cells exhaust nutrients and require passaging them to new plates. However, to exclude the possibility of cell death and support the hypothesis that cells proliferate but not in the same range as cells grown in complete growth media, we performed an assay for PI-positive cell counting by Flow Cytometry assay (Figure 6).

As is seen from Figure 6, PI-positive cells rate relatively the same for both conditions at the critical timeline of 24h, which show that cells have a strong survival response during serum deprivation and slow down their growth rate but not inducing apoptosis.

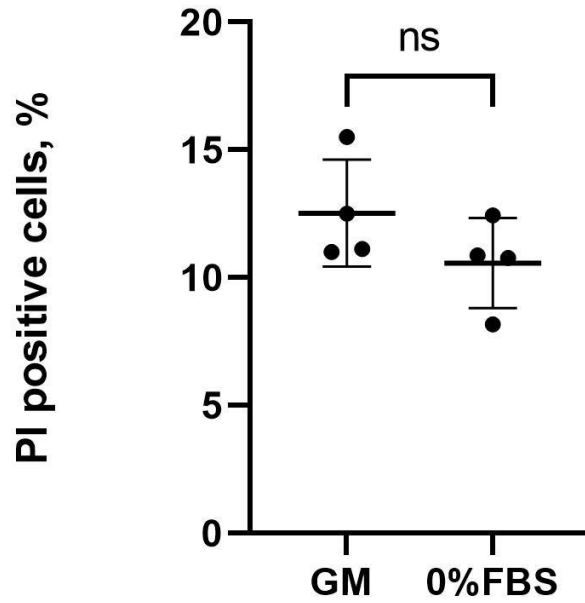


Figure 6. PI-positive cell percentage of A549 cells by Flow Cytometry assay, (24hrs, ns; not significant, Unpaired t-test).

Data was generated in triplicate, and according to the unpaired t-test the difference between results of two groups is statistically not significant (Figure 6). Also, this could be seen by cells number during 48 and 72h because they reached high numbers rather than 24h but could not reach the numbers of cells grown in full DMEM/F-12 (Figure 5). Moreover, starting from 24h, there is a correlation that cells grown in DMEM/F-12 medium without serum starts decreasing in cell size. Moreover, the same assay was done for non-KRAS HeLa cells, where comparison of cell death percentage between two groups showed statistically significant results according to the unpaired t-test (Figure 7).

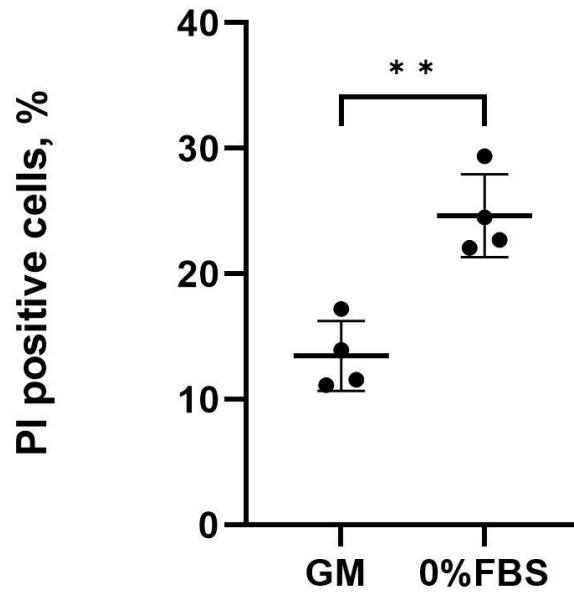
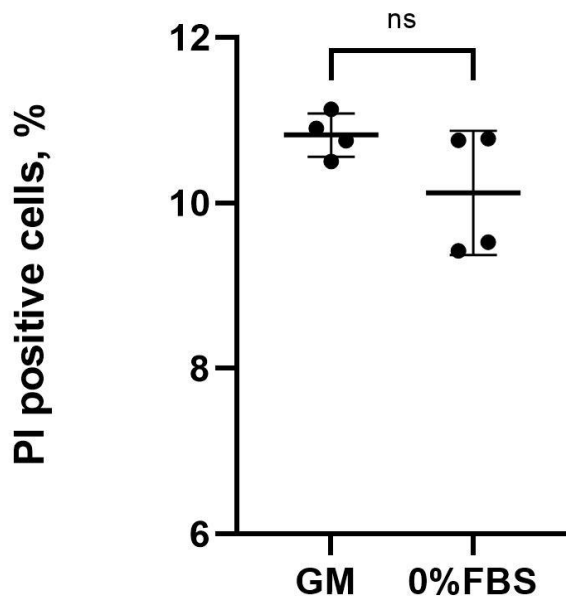


Figure 7. PI-positive cell percentage of HeLa cells by Flow Cytometry assay, (24hrs,**; $p < 0.01$, Unpaired t-test).

To be sure that this pattern in A549 cells could be continue at 48h, we performed flow cytometry assay for 48h time point for A549 cells along with HeLa cells (Figure 8). Based on the results, A549 cells did not show the high PI positive percentage, the results were the same as for complete media cells, while HeLa results become more significant in comparison with 24h, and the dead cells rate increased for serum deprived cells.

A)



B)

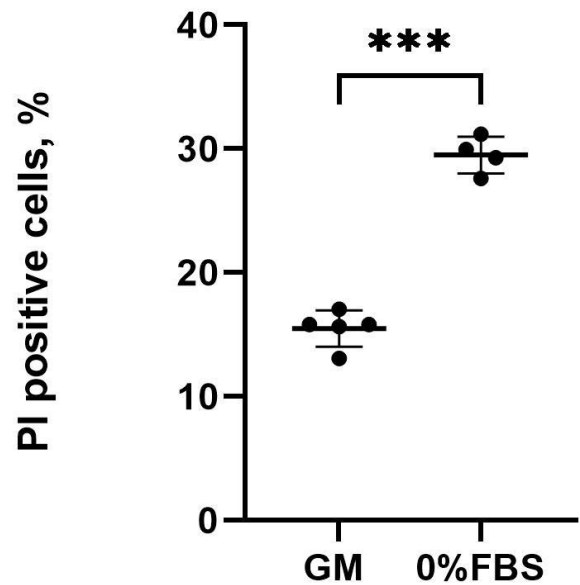


Figure 8. Flow cytometry results for A549 (A) and HeLa (B) cells at 48h in complete GM with FBS and without FBS. Cell death detected by PI staining positive cell percentage. (48hrs, ns; not significant, ***; $p < 0.001$, Unpaired t-test).

These results again indicate that A549 KRAS mutant cancer cells have a resistant response for serum deprivation, and need investigation at biochemistry level to expand understanding of process lies behind this.

3.2. Biochemistry analysis results

To evaluate changes in gene expression of cells under serum deprivation, we performed the transcriptomic studies of the total RNA fractions and also RNAs isolated from the polysome fractions (polysomal profiling). In parallel with the total RNA fractions, the polysomal fractions were analyzed to define actively translated mRNAs. The polysomal fractions were obtained by a sucrose gradient fractionation of the cytoplasmic fractions of studied cells. We carried out the fractionation with a continuous monitoring of RNA absorbance to isolate ribosomal (RNP) complexes by detecting 40S, 60S, 80S and polysomal fractions resolved on the sucrose gradient (0-60% sucrose gradient). The Biocomp Gradient Station linked to the TriaxFlow Cell (with absorbance of UV light for RNA detection) was highly effective in detection ribosomal/polysomal fractions and their isolation. It shows UV absorbance values at Y-axis, and fraction numbers at the X-axis (Figure 9). The ribosomal/polysomal profiling study of complexes in serum deprived condition did show any substantial changes in abundance of polysomal fractions (represented by the fractions #23 to #27) opposing the effects of glucose or amino acid deprived conditions associated with a substantial

decrease of polysomal fractions (the Supplementary Figure 3 and 4). The only observed a slight decrease of 80S peak (represented by the fractions #16 to #19) might be explained by compensation of a slight increase of the polysomal fraction under serum deprivation. Our study clearly indicates that a serum depletion for 24h results in active protein synthesis comparable with growth conditions (GM) and it is possible that cells adapt to serum deprivation by enhancing the set of genes required for adaptation and maintaining cell growth under serum deprived conditions (Figure 9). We propose that the transcriptomic study will be instrumental to address our hypothesis.

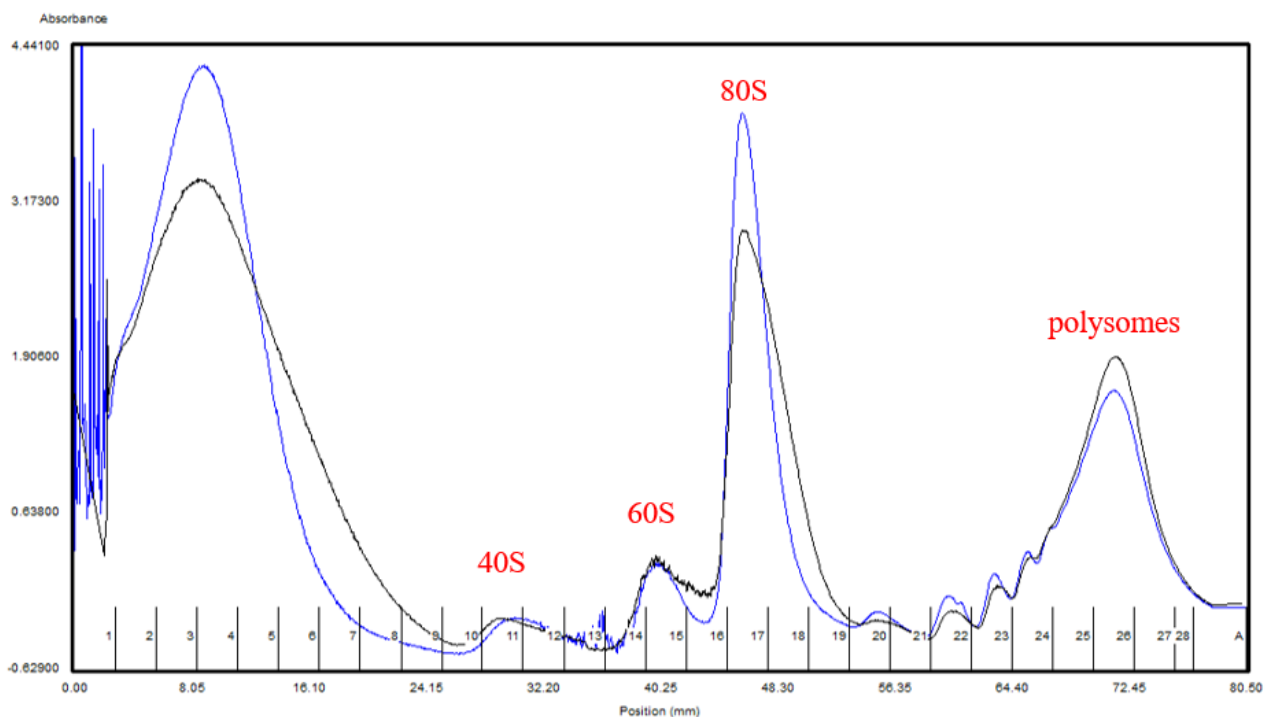


Figure 9. The ribosome/polysome profiling of A549 cancer cells incubated for 24h with serum (10% FBS) represented by blue line or without serum represented by the black line in the graph.

An observed strong adaptive response to serum deprivation is likely linked to the oncogenic KRAS expression in A549 cells because we did not observe this effect in non KRAS mutant cancer cells HeLa (Figure 10). According to this Figure 10, it is visible that polysomal fraction pick of lysates obtained from serum deprived cells (blue line) is dropped in comparison with lysates obtained from complete media (black line). Also, we did not observe it in non-cancerous cells HEK-293, which are human embryogenic kidney cells (the Supplementary Figure 5). It can be further interpreted that a nutrient deprivation has a major inhibitory impact on mTOR signaling leading to a suppression of active protein synthesis (a decrease of polysomal fractions), but it is likely that mTOR signaling

remains active under serum deprivation because an oncogenic KRAS is capable to maintain growth factor and subsequently a Rheb-dependent mTOR signaling.

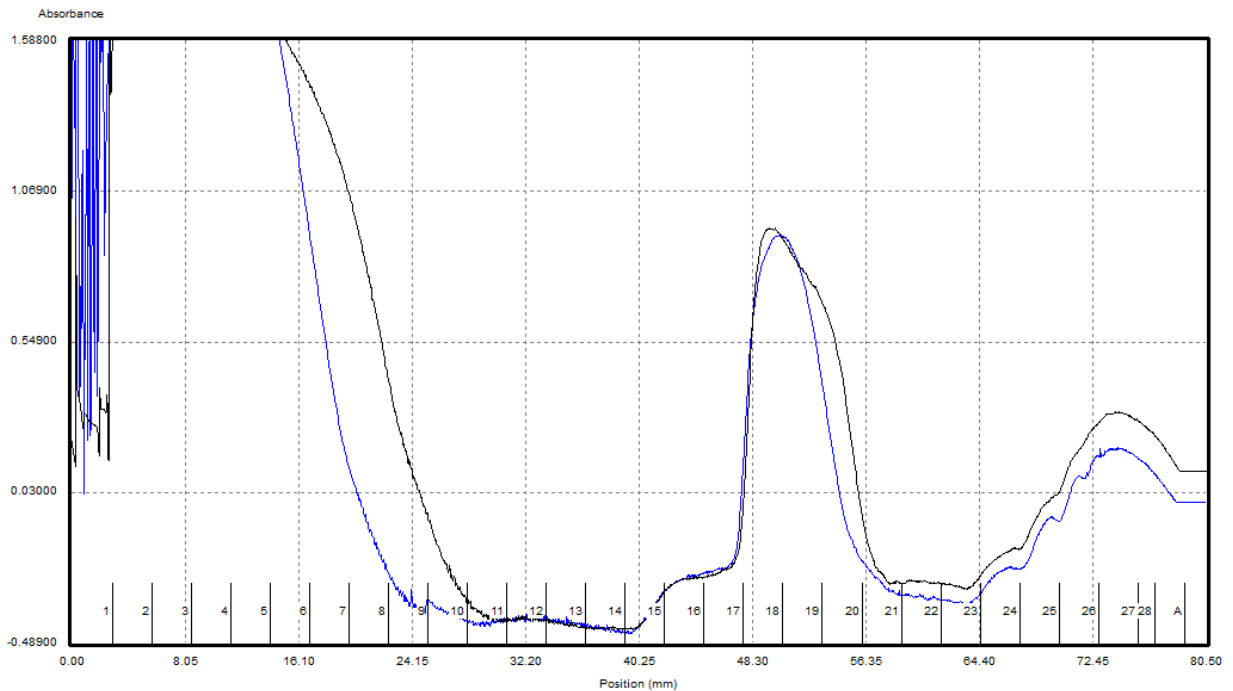


Figure 10. The ribosome/polysome profiling of HeLa cancer cells incubated for 24h with serum (10% FBS) represented by black line or without serum represented by the blue line in the graph

3.3. NGS sequencing and gene analysis results

The transcriptomic studies of mRNAs obtained from the total RNA, 80S and polysomal fractions were performed by the NGS sequencing platform by the Genomic Laboratory of NLA (National Laboratory of Astana) and analyzed by its Bioinformatic group using STAR methodology to make alignments, where differentially expressed genes were calculated through the DESeq pipeline. Validation of gene lists by enrichment analysis and pathway analysis was performed through the KEGG Database, while sample analysis and data dimensionality reduction were completed by Principal Component Analysis. Two sets of samples from A549 lung cancer cell were used in study with following conditions: GM (growth media) with 10% serum supplement and medium without Fetal Bovine Serum (key growth factor). Each set of conditions composed of RNA isolated from 80S and polysomal fractions, along with total RNAs. According to the sequencing data, we observed 294 downregulated genes and 128 overexpressed genes in 80S fractions obtained from cells that were kept in serum deprived medium. However, in the same condition in polysomes twice more

upregulated genes were shown in comparison with downregulated genes, 1482 and 611, respectively. This pattern correlates with graphs representing the RNP peaks from the last paragraph, where 80S peak dropped in comparison with polysomes (Figure 9). This sequencing allows us to hypothesize about construction of modified ribosomes in polysomes. Therefore, we identified a cluster of genes that were overexpressed in polysomal fraction according to the results of NGS analysis. (Figure 11, Table 1).

Gene name	Gene expression in complete media (control)	Gene overexpression in serum deprivation	Fold change (Log2)
ACAT2	11961.325	47290.942	1.983
FASN	4182.89	25756.028	2.6

Table 1. A quantitative representation of mRNA of FASN and ACAT2 genes associated with the polysomal fractions.

Table 1 represents gene overexpression in first two columns that given by number of reads which tells about the intensity of detected mRNA per sample, however difference of change between conditions is given in log base 2-fold change. First column represents number of mRNA reads for samples from complete media condition, while second represents serum deprived one. The value in third column obtained by division of second column to first in order to check the difference between to condition. Obtained value was calculated for log base 2, so the difference in third column represented as log base 2 ratio. This approach makes analysis and graphs more convenient for further studies. According to Figure 8, the quantitative data shows overexpressed genes labelled with red colour on the top of the heat map (Figure 11) in polysomal fractions from cells that were grown in medium without addition of fetal bovine serum. These genes are related to cholesterol and fatty acid synthesis pathways. It is likely that these genes help to cells to survive under the FBS-deprived condition through mimicking FBS environment for cells by producing more lipids. However, we decided to focus on two genes that involved in regulation of central lipid pathway, which are not included in our heatmap, but presented in excel data file (Table 1). To validate the NGS data, we performed the Q-PCR analysis by designed specific primers for detection of the critical cholesterol and fatty acid synthesis mRNA abundance of Acetyl-CoA Acetyltransferase 2 (ACAT2) gene, and the fatty acid synthesis-related gene FASN, which only one highly overexpressed fatty acid pathway gene (Table 2S). FASN is multifunctional enzyme with several domains, which include ketoacyl synthase, but for this work seems interesting particularly its role in lipid biosynthesis. According to the published papers, FASN is a key enzyme that associated with lipid biosynthesis, acting as a

substrate to producing energy since highly involved in production of ATP and free fatty acids [37]. Thereby, becoming influential for cancer cells, and probably playing an important role in survival of cancer under the various nutrient and metabolic stress conditions. The second gene ACAT2 is also essential since it participates in mevalonate pathway by synthesizing acetoacetyl, acting through its enzymatic domain acyltransferase domain. ACAT2 is basal for cholesterol and important intermediate in fatty acid synthesis. ACAT2 can be considered as an important enzyme in cholesterol pathway [38] because ACAT2 enzyme involved in such process, called esterification of cholesterol, which make possible transformation of cholesterol into cholesterol esters, this makes possible storage of cholesterol within cells, providing cell with the needed amount of lipid, etc. [39]. Supporting our hypothesis that overexpressed genes probably play role in adaptation to serum deprivation in A549 cancer cells, which in normal condition use serum as a source of lipids.

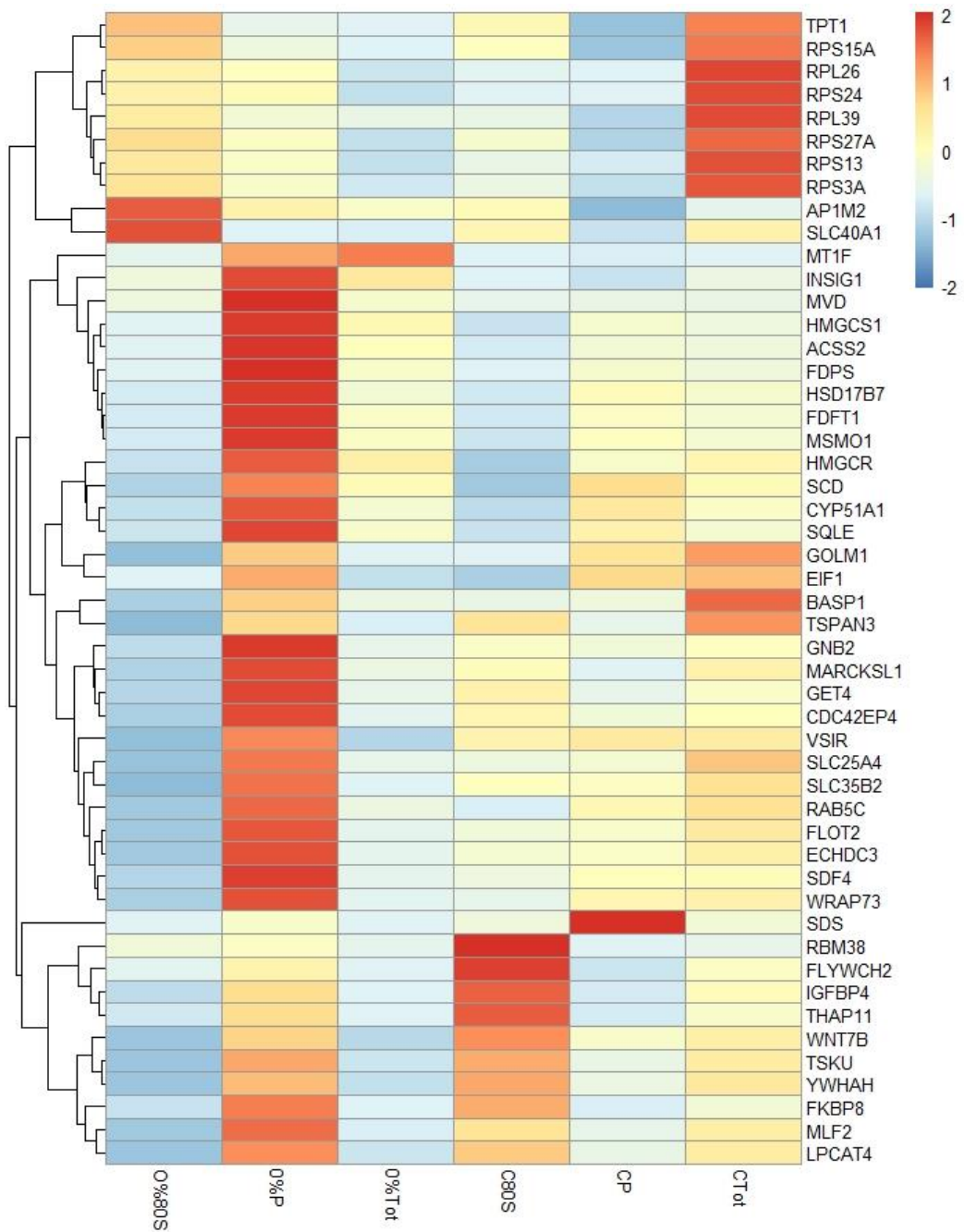


Figure 11. The heatmap of transcriptomic analysis of polysomal and 80S fractions from serum deprived conditions and GM. All samples labeled with 0% on the bottom of X-axis are FBS deprived conditions, while Y-axis shows the genes that overexpressed.

3.4. Functional analysis

3.4.1 Conventional PCR based

Based on the NGS sequencing results, the detected ACAT2 and FASN mRNAs could represent the functionally essential genes for KRAS mutant cancer cells survival under serum deprived conditions. It might explain the serum-independent survival and growth mechanisms of cancer cells. As mentioned in the previous section, most of the overexpressed genes are related to the cholesterol synthesis and fatty acid synthesis gene clusters. From that cluster, we chose to present in this study cholesterol-related gene (ACAT2) gene, and the fatty acid synthesis-related gene FASN, which also showed a high overexpression rate. As mentioned in the previous chapter primers for this experiment were designed through the NCBI Primer Blast tool (<https://www.ncbi.nlm.nih.gov/tools/primer-blast/>) and presented in Table 2S. PCR reaction was followed according to the protocol described in the methodology part with a common annealing temperature (52 °C), which was set according to the primer characteristics. The distinct DNA bands corresponding to the expected PCR product size were detected (Figure 12). The expected product size for FASN was 222 bp, while for ACAT2 it was 243 bp, which corresponds to the amplified DNA bands in agarose gel electrophoresis. As an internal control, we used 18S rDNA, it is an abundant RNA, and most reliable control for a qPCR performance. We isolated RNA samples from the total and polysomal fractions of A549 cells incubated with or without serum.

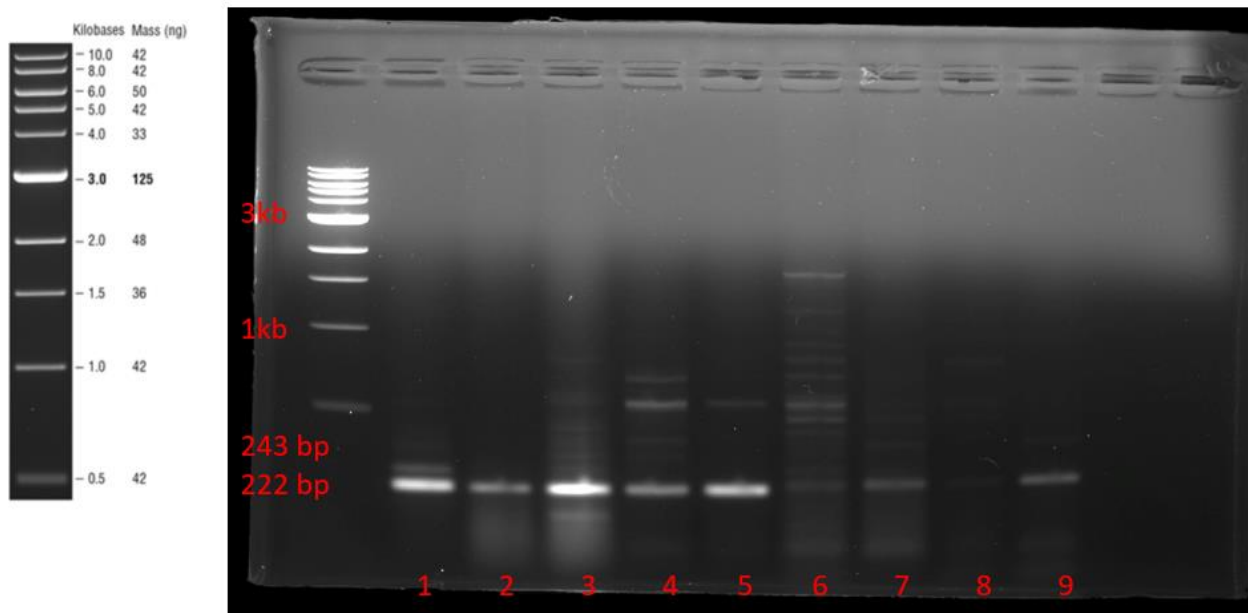


Figure 12. Agarose gel electrophoresis for target genes FASN and ACAT2. (1) 18S rDNA Control conditions; (2) FASN control total; (3) FASN 0FBS total; (4) FASN control polysomal; (5) FASN 0FBS polysomal; (6) ACAT2 control total; (7) ACAT2 0FBS total; (8) ACAT2 control (control) polysomal; (9) ACAT2 0FBS polysomal.

3.4.2 RT-qPCR-based validation

RT-qPCR assay was used to measure the expression levels of ACAT2 and FASN genes. As was described in the methodology part, RNAs from total lysate, 80S and polysomal fraction were extracted and reverse transcribed according to the Applied Biosystems protocol. The expression level was detected by qPCR in samples according isolation from A549 cells for both conditions, Control and FBS deprived cells. Unfortunately, below results present only expression levels for total RNA templates, reasons for that will be explained in details in limitation part. According to the results of qPCR (Figure 13, Table 2) FASN gene show reaction curve, which pass threshold line at the early Cq value. However, we could not able to say exactly is it higher than the control sample since we were not able to obtain curve that will pass the threshold. In this case, we are not excluding pipetting error that also possible. In contrast, we had another control cDNA template where we observed late threshold intersection than in comparison with FASN amplification for FBS-deprived template.

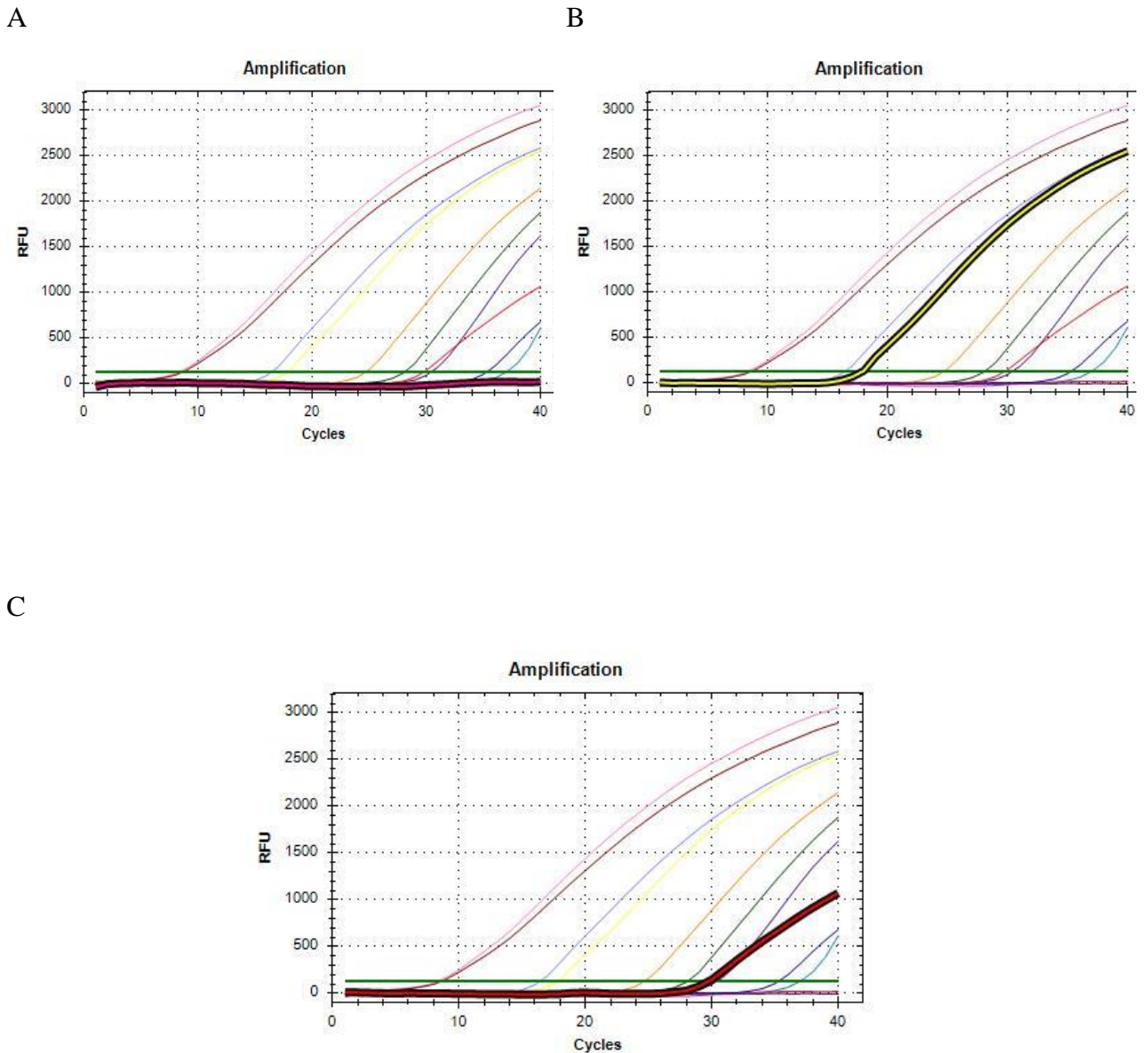


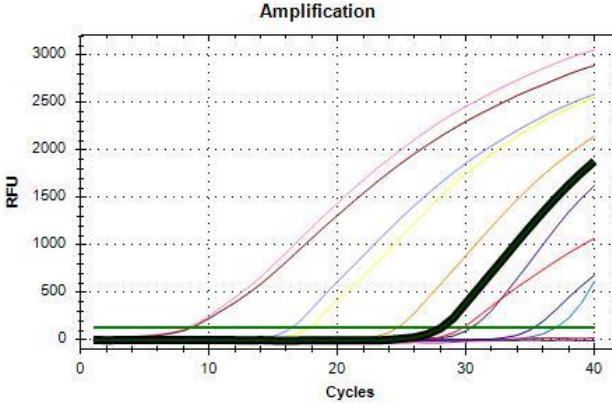
Figure 13. Representation of qPCR amplification for FASN gene. Curves for the conditions are bold. (A) FASN amplification for control total RNA; (B) FASN amplification for FBS deprived total RNA; (C) nonspecific control cDNA.

Gene	Cq value (number of cycles)
FASN control (GM sample)	0
FASN 0%FBS (serum deprived)	17.91
FASN non-specific cDNA control	29.75

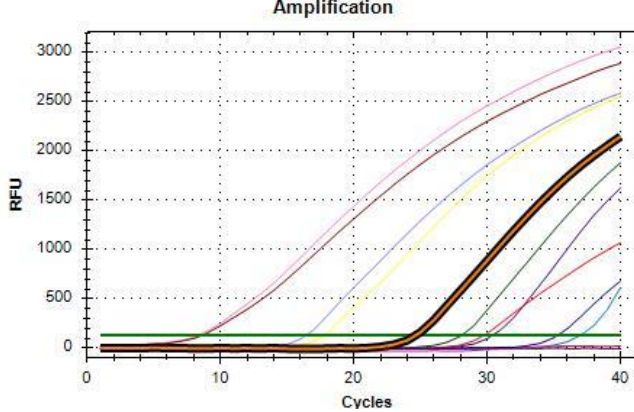
Table 2. Representation of Cq values f FASN gene depends on a cDNA sample type

For ACAT2 gene amplification we get slightly early threshold pass for FBS-deprived template, but margin between control and FBS-deprived template was not so critic (Figure 14, Table 3). The same pattern we obtained with nonspecific cDNA template that used as a control like in previous case, late intersection of threshold. As it known, if during amplification sample intersect threshold at early stages, it means there is more expression in comparison with others. This intersection point gives as Cq values, which is represent the number of cycles needed to pass threshold. Overall, we see the correlation with NGS results, where both genes were overexpressed in every mRNA sample for FBS-deprived condition. However, it is hard to make solid conclusion since data is not in triplicate, we are in progress to obtain that.

A



B



C

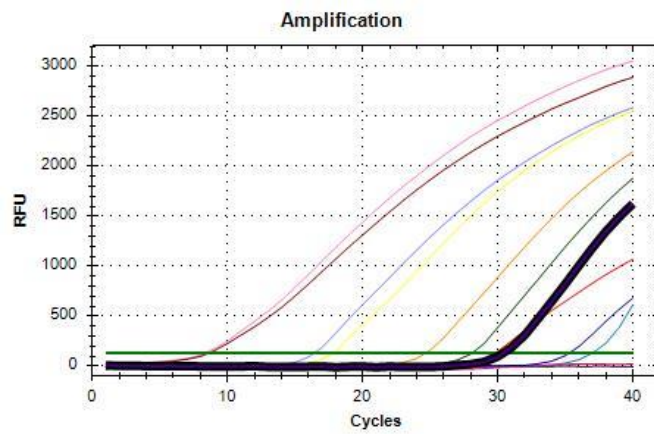


Figure 14. Representation of qPCR amplification for ACAT2 gene. Curves for the conditions are bold. (A) ACAT2 amplification for control total RNA; (B) ACAT2 amplification for FBS deprived total RNA; (C) nonspecific control cDNA.

Gene	Cq value (number of cycles)
ACAT2 control (GM sample)	28.09
ACAT2 0%FBS (serum deprived)	24.62
ACAT2 non-specific cDNA control	30.38

Table 3. Representation of Cq values of FASN gene depends on a cDNA sample type.

4 Discussion

In recent decades, cancer-related research becomes widely investigated from the angle of fundamental studies in biochemistry to understand the process that lies behind such as the aggressive proliferation or sensitivity of cancer cells to any metabolic stress. An increasing number of research investigating the metabolic stress of cancer cells caused by nutrient deprivation [12], [37], [38], [39] since the tissue culture conditions were created to mimic the *in vivo* cases. Along with nutrient deprivation studies [14], the bulk of investigations in this decade push the workflow to understand the effect of fetal bovine serum (FBS) on cancer cells [22]. However, this research area remains arguable since it is not well described how FBS affect cancer cells, and through which biochemical mechanisms it is regulated. Moreover, as was mentioned in the introduction, some of the research have controversial points with each other, which complicates the development of solid conclusions about the implications, and the role of FBS in cancer research. Apart from that, the scientific community is concerned about the high price of this supplement and the possibility to produce misleading results. Published literatures mostly focused on proliferation rates of cell under FBS-deprivation or on expression of particular important proteins for cancer survival [20], but there are almost no papers that check the ribosomal profile, or gene expression changes at the NGS level for cancer cells during FBS-deprivation. Taking into consideration, we decided to fill this gap in this study and to understand how actually FBS-deprivation may affect KRAS mutant cancer cell line on gene expression level and change its ribosomal profile.

Based on results presented in the previous chapter, A549 cancer cell lines have slightly dropped in their growth rate and cell size during serum deprivation, which is opposite for some reports of previous publications that points out FBS as an essential supplement for the cell survival. However, our results also support the rest of the studies suggesting slightly drop of proliferation, but still high resistance for deprivation of this component, which could be explained by the molecular processes. Since the main focus of this study was to understand biochemical changes under this condition, we did the 80S/polysome complexes profile of the cells. According to the experience of published literature, where nutrient deprivation and ribosomal biogenesis were discussed [40], we expected that during deprivation of FBS, cells will be unable to accumulate RNP complexes and proteins under the high level. However, as it was shown in results, we reach opposite data, where polysome complex was overexpressed in comparison with normal conditions, and despite the less energy supply under the deprived condition cells were able to maintain workflow of multiple ribosomes to translate mRNA template to produce efficiently more proteins. This reproducible data pushed us to deeply investigate, what was translated, and which genes get overexpressed to produce more proteins.

To approve our hypothesis that under the FBS-deprived condition, KRAS mutant cancer cells start translating particular proteins through which they probably adapt, we send our samples for NGS and obtain transcriptome data. Results of analysing transcriptome data showed that under the FBS-deprived conditions in polysome RNP complex cholesterol synthesis related genes such as ACAT2, HMGCR are overexpressed. Despite the clear consensus on the role of cholesterol synthesis related genes in cells, especially in cancer cell, it is still unclear through which particular axes of cellular pathway they are regulated. It has been shown that [41] cholesterol synthesis potential therapeutic target for glioblastoma cancer type due to ethiology of the disease itself, since cholesterol start being accumulated in the brain. Also, some paper [42] reported the cancer cell death during inhibition of cholesterol synthesis with specific drugs, and proposed that this apoptotic processes regulated by small Rho GTPases. This point support our hypothesis that resistance to the serum deprivation is intrinsic only for KRAS mutant cancer cells. However, it is still point of debate, how cholesterol pathway regulated in FBS deprived cancer cell lines, through which mutually exclusive cellular pathway axes it is get orchestrated and lead to cell survival. We propose that this adaptation happens by indirect regulation of mTORC1 complex through the upstream regulators since the sterol regulatory element-binding protein (SREBP), which activates genes involved in cholesterol synthesis, is a downstream target of the mTOR. Therefore, there is a possibility that inhibition of SREBP could be lethal for cells without causing FBS deprivation, however, it is already known that MAPK and AKT pathway inhibition lead to blockage of KRAS-mutant cancer cells [43], [44], [45], [46], [47], [48]. There is a plenty of alternatives that possibly will inhibit KRAS mutation, but further continuation of this study aimed to understand how it possible based on our findings, and what is the biological mechanism behind that.

Summary

In this work we assessed the KRAS mutant cancer cell response for the FBS deprived condition (i), and identified that cancer cells dropped proliferation rate, not enter apoptotic stage. Based on that we provided a biochemical studies, where clearly show that polysome RNP complex show overexpressed picks (ii) signaling about functional relevance of translated proteins. In order to approve this we made NGS for isolated sample, and identified that cholesterol-related genes plays a central role in adaptation of cancer cell lines for FBS-deprived condition (iii), which is support broad tissue culture rule that FBS one of the key supplement for cell maintenance, and on the contrary the improper usage of which could lead to misleading results.

6 Limitations

This study carries several limitations. Firstly, NGS analyzing was not done in triplicate since the preparation samples is time consuming process, while procedure itself is expensive, and need high quality sample preparation at once. Due to this reason also, we did not provide control cell line to this experiment. Moreover, main objective of this research was to show and investigate the effect of serum deprivation particularly on cancer cells since it is not a drug treatment response testing. However, if further question will move to the commercial relevance of the project such as saving money for laboratories on FBS, considering control non cancer line is important for us. Regarding the last experiment RT- qPCR, results are not presented in triplicates since our reagents run out, and find from our collaborators were hard since it is expensive and important reagents, and all of us facing troubles with logistic in order to transfer them into Kazakhstan. Also, data presented for this experiment belong for the total RNA samples, not for polysome, that is why couldn't be the source of entire conclusion. Nevertheless, all these problems will be fixed in the paper that we want to publish within this project.

Bibliography

1. World Health Organization. WHO report on cancer: setting priorities, investing wisely and providing care for all; 2020.
2. Sakamoto H, Attiyeh MA, Gerold JM, Makohon-Moore AP, Hayashi A, Hong J, Kappagantula R, Zhang L, Melchor JP, Reiter JG, Heyde A, Bielski CM, Penson AV, Gönen M, Chakravarty D, O'Reilly EM, Wood LD, Hruban RH, Nowak MA, Socci ND, Taylor BS, Iacobuzio-Donahue CA. The Evolutionary Origins of Recurrent Pancreatic Cancer. *Cancer Discov.* 2020 Jun;10(6):792-805. doi: 10.1158/2159-8290.CD-19-1508. Epub 2020 Mar 19. PMID: 32193223; PMCID: PMC7323937.
3. Buscail L, Bournet B, Cordelier P. Role of oncogenic KRAS in the diagnosis, prognosis and treatment of pancreatic cancer. *Nat Rev Gastroenterol Hepatol.* 2020 Mar;17(3):153-168. doi: 10.1038/s41575-019-0245-4. Epub 2020 Jan 31. PMID: 32005945.
4. Kerr EM, Martins CP. Metabolic rewiring in mutant Kras lung cancer. *FEBS J.* 2018 Jan;285(1):28-41. doi: 10.1111/febs.14125. Epub 2017 Jun 22. PMID: 28570035; PMCID: PMC6005344.
5. Kawada K, Toda K, Sakai Y. Targeting metabolic reprogramming in KRAS-driven cancers. *Int J Clin Oncol.* 2017 Aug;22(4):651-659. doi: 10.1007/s10147-017-1156-4. Epub 2017 Jun 24. PMID: 28647837.
6. Waters AM, Der CJ. KRAS: The Critical Driver and Therapeutic Target for Pancreatic Cancer. *Cold Spring Harb Perspect Med.* 2018 Sep 4;8(9): a031435. doi: 10.1101/cshperspect.a031435. PMID: 29229669; PMCID: PMC5995645.
7. Burska, A. N., Ilyassova, B., Dildabek, A., Khamijan, M., Begimbetova, D., Molnár, F., & Sarbassov, D. D. (2022). Enhancing an Oxidative “Trojan Horse” Action of Vitamin C with Arsenic Trioxide for Effective Suppression of KRAS-Mutant Cancers: A Promising Path at the Bedside. *Cells*, 11(21), 3454.
8. Weinberg F, Hamanaka R, Wheaton WW, Weinberg S, Joseph J, Lopez M, Kalyanaraman B, Mutlu GM, Budinger GR, Chandel NS. Mitochondrial metabolism and ROS generation are essential for Kras-mediated tumorigenicity. *Proc Natl Acad Sci U S A.* 2010 May 11;107(19):8788-93. doi: 10.1073/pnas.1003428107. Epub 2010 Apr 26. PMID: 20421486; PMCID: PMC2889315.
9. Hanahan D. Hallmarks of Cancer: New Dimensions. *Cancer Discov.* 2022 Jan;12(1):31-46. doi: 10.1158/2159-8290.CD-21-1059. PMID: 35022204.
10. Hanahan D, Weinberg RA. Hallmarks of cancer: the next generation. *Cell.* 2011 Mar 4;144(5):646-74. doi: 10.1016/j.cell.2011.02.013. PMID: 21376230.
11. Altea-Manzano P, Cuadros AM, Broadfield LA, Fendt SM. Nutrient metabolism and cancer in the in vivo context: a metabolic game of give and take. *EMBO Rep.* 2020 Oct 5;21(10):e50635. doi:

- 10.15252/embr.202050635. Epub 2020 Sep 23. PMID: 32964587; PMCID: PMC7534637.
12. Selwan EM, Finicle BT, Kim SM, Edinger AL. Attacking the supply wagons to starve cancer cells to death. *FEBS Lett.* 2016 Apr;590(7):885-907. doi: 10.1002/1873-3468.12121. Epub 2016 Mar 22. PMID: 26938658; PMCID: PMC4833639.
13. Aubert L, Nandagopal N, Roux PP. Targeting copper metabolism to defeat KRAS-driven colorectal cancer. *Mol Cell Oncol.* 2020 Oct 7;7(6):1822123. doi: 10.1080/23723556.2020.1822123. PMID: 33235918; PMCID: PMC7671051.
14. Liu YH, Hu CM, Hsu YS, Lee WH. Interplays of glucose metabolism and KRAS mutation in pancreatic ductal adenocarcinoma. *Cell Death Dis.* 2022 Sep 24;13(9):817. doi: 10.1038/s41419-022-05259-w. PMID: 36151074; PMCID: PMC9508091.
15. Faubert B, Solmonson A, DeBerardinis RJ. Metabolic reprogramming and cancer progression. *Science.* 2020 Apr 10;368(6487):eaaw5473. doi: 10.1126/science.aaw5473. PMID: 32273439; PMCID: PMC7227780.
16. Ricoult SJ, Yecies JL, Ben-Sahra I, Manning BD. Oncogenic PI3K and K-Ras stimulate de novo lipid synthesis through mTORC1 and SREBP. *Oncogene.* 2016 Mar 10;35(10):1250-60. doi: 10.1038/onc.2015.179. Epub 2015 Jun 1. PMID: 26028026; PMCID: PMC4666838.
17. Singh A, Ruiz C, Bhalla K, Haley JA, Li QK, Acquah-Mensah G, Montal E, Sudini KR, Skoulidis F, Wistuba II, Papadimitrakopoulou V, Heymach JV, Boros LG, Gabrielson E, Carretero J, Wong KK, Haley JD, Biswal S, Girnun GD. De novo lipogenesis represents a therapeutic target in mutant Kras non-small cell lung cancer. *FASEB J.* 2018 Jun 15;32(12):fj201800204. doi: 10.1096/fj.201800204. Epub ahead of print. PMID: 29906244; PMCID: PMC6219836.
18. Wong CC, Wu JL, Ji F, Kang W, Bian X, Chen H, Chan LS, Luk STY, Tong S, Xu J, Zhou Q, Liu D, Su H, Gou H, Cheung AH, To KF, Cai Z, Shay JW, Yu J. The cholesterol uptake regulator PCSK9 promotes and is a therapeutic target in APC/KRAS-mutant colorectal cancer. *Nat Commun.* 2022 Jul 8;13(1):3971. doi: 10.1038/s41467-022-31663-z. PMID: 35803966; PMCID: PMC9270407.
19. Cheng, Hui, Meng Wang, Jingjing Su, Yueyue Li, Jiao Long, Jing Chu, Xinyu Wan, Yu Cao, and Qinglin Li. 2022. "Lipid Metabolism and Cancer" *Life* 12, no. 6: 784. <https://doi.org/10.3390/life12060784>
20. Rashid MU, Coombs KM. Serum-reduced media impacts on cell viability and protein expression in human lung epithelial cells. *J Cell Physiol.* 2019 Jun;234(6):7718-7724. doi: 10.1002/jcp.27890. Epub 2018 Dec 4. PMID: 30515823; PMCID: PMC6519280.
21. Pirkmajer S, Chibalin AV. Serum starvation: caveat emptor. *Am J Physiol Cell Physiol.* 2011 Aug;301(2):C272-9. doi: 10.1152/ajpcell.00091.2011. Epub 2011 May 25. PMID: 21613612.
22. White EZ, Pennant NM, Carter JR, Hawsawi O, Odero-Marah V, Hinton CV. Serum deprivation initiates adaptation and survival to oxidative stress in prostate cancer cells. *Sci Rep.* 2020 Jul 27;10(1):12505. doi: 10.1038/s41598-020-68668-x. PMID: 32719369; PMCID: PMC7385110.
23. Huang Y, Fu Z, Dong W, Zhang Z, Mu J, Zhang J. Serum starvation-induces down-regulation of Bcl-2/Bax confers apoptosis in tongue coating-related cells in vitro. *Mol Med Rep.* 2018

Apr;17(4):5057-5064. doi: 10.3892/mmr.2018.8512. Epub 2018 Jan 29. PMID: 29393442; PMCID: PMC5865968.

24. Ni P, Xu H, Chen C, Wang J, Liu X, Hu Y, Fan Q, Hou Z, Lu Y. Serum starvation induces DRAM expression in liver cancer cells via histone modifications within its promoter locus. *PLoS One*. 2012;7(12):e50502. doi: 10.1371/journal.pone.0050502. Epub 2012 Dec 12. PMID: 23251372; PMCID: PMC3520922.

25. Levin VA, Panchabhai SC, Shen L, Kornblau SM, Qiu Y, Baggerly KA. Different changes in protein and phosphoprotein levels result from serum starvation of high-grade glioma and adenocarcinoma cell lines. *J Proteome Res*. 2010 Jan;9(1):179-91. doi: 10.1021/pr900392b. PMID: 19894763; PMCID: PMC3386607.

26. Ibrahim SAE, Abudu A, Johnson E, Aftab N, Conrad S, Fluck M. The role of AP-1 in self-sufficient proliferation and migration of cancer cells and its potential impact on an autocrine/paracrine loop. *Oncotarget*. 2018 Sep 28;9(76):34259-34278. doi: 10.18632/oncotarget.26047. Erratum in: *Oncotarget*. 2019 Jan 22;10(7):799. Jonhson, Eugenia [corrected to Johnson, Eugenia]. PMID: 30344941; PMCID: PMC6188139.

27. McKnight BN, Kim S, Boerner JL, Viola NT. Cetuximab PET delineated changes in cellular distribution of EGFR upon dasatinib treatment in triple negative breast cancer. *Breast Cancer Res*. 2020 Apr 15;22(1):37. doi: 10.1186/s13058-020-01270-1. PMID: 32295603; PMCID: PMC7160960.

28. Harachi M, Masui K, Okamura Y, Tsukui R, Mischel PS, Shibata N. mTOR Complexes as a Nutrient Sensor for Driving Cancer Progression. *Int J Mol Sci*. 2018 Oct 21;19(10):3267. doi: 10.3390/ijms19103267. PMID: 30347859; PMCID: PMC6214109.

29. Abetov DA, Kiyani VS, Zhylykbayev AA, Sarbassova DA, Alybayev SD, Spooner E, Song MS, Bersimbaev RI, Sarbassov DD. Formation of mammalian preribosomes proceeds from intermediate to composed state during ribosome maturation. *J Biol Chem*. 2019 Jul 12;294(28):10746-10757. doi: 10.1074/jbc.AC119.008378. Epub 2019 May 10. PMID: 31076509; PMCID: PMC6635442.

30. Pecoraro A, Pagano M, Russo G, Russo A. Ribosome Biogenesis and Cancer: Overview on Ribosomal Proteins. *Int J Mol Sci*. 2021 May 23;22(11):5496. doi: 10.3390/ijms22115496. PMID: 34071057; PMCID: PMC8197113.

31. Haque A, Engel J, Teichmann SA, Lönnberg T. A practical guide to single-cell RNA-sequencing for biomedical research and clinical applications. *Genome Med*. 2017 Aug 18;9(1):75. doi: 10.1186/s13073-017-0467-4. PMID: 28821273; PMCID: PMC5561556.

32. Goodall GJ, Wickramasinghe VO. RNA in cancer. *Nat Rev Cancer*. 2021 Jan;21(1):22-36. doi: 10.1038/s41568-020-00306-0. Epub 2020 Oct 20. PMID: 33082563.

33. Cavicchioli MV, Santorsola M, Balboni N, Mercatelli D, Giorgi FM. Prediction of Metabolic Profiles from Transcriptomics Data in Human Cancer Cell Lines. *Int J Mol Sci*. 2022 Mar 31;23(7):3867. doi: 10.3390/ijms23073867. PMID: 35409231; PMCID: PMC8998886.

34. Cieřlik M, Chinnaiyan AM. Cancer transcriptome profiling at the juncture of clinical

- translation. *Nat Rev Genet.* 2018 Feb;19(2):93-109. doi: 10.1038/nrg.2017.96. Epub 2017 Dec 27. PMID: 29279605.
35. Kok DE, O'Flanagan CH, Coleman MF, Ashkavand Z, Hursting SD, Krupenko SA. Effects of folic acid withdrawal on transcriptomic profiles in murine triple-negative breast cancer cell lines. *Biochimie.* 2020 Jun;173:114-122. doi: 10.1016/j.biochi.2020.04.005. Epub 2020 Apr 15. PMID: 32304770; PMCID: PMC7858693.
36. Seisenova A, Daniyarov A, Molkenov A, Sharip A, Zinovyev A, Kairov U. Meta-Analysis of Esophageal Cancer Transcriptomes Using Independent Component Analysis. *Front Genet.* 2021 Oct 21;12:683632. doi: 10.3389/fgene.2021.683632. PMID: 34795689; PMCID: PMC8594933.
37. Subbiahanadar Chelladurai K, Selvan Christyraj JD, Rajagopalan K, Yesudhason BV, Venkatachalam S, Mohan M, Chellathurai Vasantha N, Selvan Christyraj JRS. Alternative to FBS in animal cell culture - An overview and future perspective. *Heliyon.* 2021 Jul 28;7(8):e07686. doi: 10.1016/j.heliyon.2021.e07686. PMID: 34401573; PMCID: PMC8349753.
38. Jin K, Ewton DZ, Park S, Hu J, Friedman E. Mirk regulates the exit of colon cancer cells from quiescence. *J Biol Chem.* 2009 Aug 21;284(34):22916-25. doi: 10.1074/jbc.M109.035519. Epub 2009 Jun 19. PMID: 19542220; PMCID: PMC2755699.
39. Lee SH, Jung YS, Chung JY, Oh AY, Lee SJ, Choi DH, Jang SM, Jang KS, Paik SS, Ha NC, Park BJ. Novel tumor suppressive function of Smad4 in serum starvation-induced cell death through PAK1-PUMA pathway. *Cell Death Dis.* 2011 Dec 1;2(12):e235. doi: 10.1038/cddis.2011.116. PMID: 22130069; PMCID: PMC3252743.
40. Jo H, Jia Y, Subramanian KK, Hattori H, Luo HR. Cancer cell-derived clusterin modulates the phosphatidylinositol 3'-kinase-Akt pathway through attenuation of insulin-like growth factor 1 during serum deprivation. *Mol Cell Biol.* 2008 Jul;28(13):4285-99. doi: 10.1128/MCB.01240-07. Epub 2008 May 5. PMID: 18458059; PMCID: PMC2447147.
- 41 Chang L, Fang S, Chen Y, Yang Z, Yuan Y, Zhang J, Ye L, Gu W. Inhibition of FASN suppresses the malignant biological behavior of non-small cell lung cancer cells via deregulating glucose metabolism and AKT/ERK pathway. *Lipids Health Dis.* 2019 May 24;18(1):118. doi: 10.1186/s12944-019-1058-8. PMID: 31122252; PMCID: PMC6533754.
- 42 Brandi J, Dando I, Pozza ED, Biondani G, Jenkins R, Elliott V, Park K, Fanelli G, Zolla L, Costello E, Scarpa A, Cecconi D, Palmieri M. Proteomic analysis of pancreatic cancer stem cells: Functional role of fatty acid synthesis and mevalonate pathways. *J Proteomics.* 2017 Jan 6;150:310-322. doi: 10.1016/j.jprot.2016.10.002. Epub 2016 Oct 13. PMID: 27746256.
- 43 Hai Q, Smith JD. Acyl-coenzyme A: Cholesterol acyltransferase (ACAT) in cholesterol metabolism: From its discovery to clinical trials and the Genomics Era. *Metabolites.* 2021;11(8):543.
44. Pan M, Zorbas C, Sugaya M, Ishiguro K, Kato M, Nishida M, Zhang HF, Candeias MM, Okamoto A, Ishikawa T, Soga T, Aburatani H, Sakai J, Matsumura Y, Suzuki T, Proud CG, Lafontaine DLJ, Osawa T. Glutamine deficiency in solid tumor cells confers resistance to ribosomal RNA synthesis

inhibitors. *Nat Commun.* 2022 Jun 28;13(1):3706. doi: 10.1038/s41467-022-31418-w. PMID: 35764642; PMCID: PMC9240073

45 Pirmoradi L, Seyfizadeh N, Ghavami S, Zeki AA, Shojaei S. Targeting cholesterol metabolism in glioblastoma: a new therapeutic approach in cancer therapy. *J Investig Med.* 2019 Apr;67(4):715-719. doi: 10.1136/jim-2018-000962. Epub 2019 Feb 14. PMID: 30765502.

46 Alizadeh J, Zeki AA, Mirzaei N, Tewary S, Rezaei Moghadam A, Glogowska A, Nagakannan P, Eftekharpour E, Wiechec E, Gordon JW, Xu FY, Field JT, Yoneda KY, Kenyon NJ, Hashemi M, Hatch GM, Hombach-Klonisch S, Klonisch T, Ghavami S. Mevalonate Cascade Inhibition by Simvastatin Induces the Intrinsic Apoptosis Pathway via Depletion of Isoprenoids in Tumor Cells. *Sci Rep.* 2017 Mar 27;7:44841. doi: 10.1038/srep44841. PMID: 28344327; PMCID: PMC5366866.

47 Lai H, Wang Y, Duan F, Li Y, Jiang Z, Luo L, Liu L, Leung ELH, Yao X. Krukovine Suppresses KRAS-Mutated Lung Cancer Cell Growth and Proliferation by Inhibiting the RAF-ERK Pathway and Inactivating AKT Pathway. *Front Pharmacol.* 2018 Aug 22;9:958. doi: 10.3389/fphar.2018.00958. PMID: 30186180; PMCID: PMC6113384.

48 Xie C, Li Y, Li LL, Fan XX, Wang YW, Wei CL, Liu L, Leung EL, Yao XJ. Identification of a New Potent Inhibitor Targeting KRAS in Non-small Cell Lung Cancer Cells. *Front Pharmacol.* 2017 Nov 14;8:823. doi: 10.3389/fphar.2017.00823. PMID: 29184501; PMCID: PMC5694459.

Supplemented materials

Table S1. Summary of research articles investigating serum deprivation conditions' effect on cancer cell line behavior.

Study object	Serum-deprived conditions	Treatment time	Effect	Induced mechanism	Reference
HD6 subclone of HT29 human colorectal adenocarcinoma cells	0% FBS	0-48 hours (h)	moved to Quiescent G0 State	High expression of Mirk - serine/threonine kinase	[33] Jin et al.
HCT116 colon cancer cells	0%FBS	0, 6, and 12 h	Decreased cell viability ad cell death	Induction of Smad4 tumor suppressor that lead to PUMA mediated cell's death	[34] Lee et al.
HepG2, HepB3 - hepatocellular carcinoma cell lines	0%FBS	0, 5, 15, 30 min 1, 2, 3, 24, 48 h	Apoptosis	DRAM tumor suppressor induction	[19] Ni et al. (2012)
A tongue squamous cell carcinoma cell line, Tca8113	0%FBS	12, 24, 36, 48 and 72 h	Cell cycle arrest at G1, cell death	Downregulatioi of ration Bcl-2/Bax inline with apoptosis	[18] Huang et al. (2018)
Breast cancer cell lines MDA-MB-231, MDA-MB-468 BT549, SUM149, SUM159, MCF10A.	0%FBS	8h and 48h	MDA-MB-468 and MDA-MB-231 show progress of proliferation along with	AP-1 activity and Fra-1 expression regulates the cells' high proliferation during serum starvation	[21] Ibrahim et al. (2018)

Lung cancer cell lines H2347, HCC78, A549			lung cancer lines		
HeLa - Human Epithelial adenocarcinoma	0%FBS	0.5 h - 60 h	Dormant state	AKT pathway activation by the clusterin mediation	[35] Jo et al. (2008)
Human breast cell lines (MCF7, MDA231, MDA468); Human pancreatic carcinoma (MiaPaCa); Human colon carcinoma (KM125c); Two human ovarian carcinomas (OVCAR5, SKOV3) Glioma line (LNZ308, SNB19, U87)	0.5% FBS	24h	Apoptosis Resistance to serum-deprived apoptosis	High expression rates of apoptotic proteins	[20] Levin et al. (2010)

Table S2. Table Primers for identification of cholesterol pathway specific genes

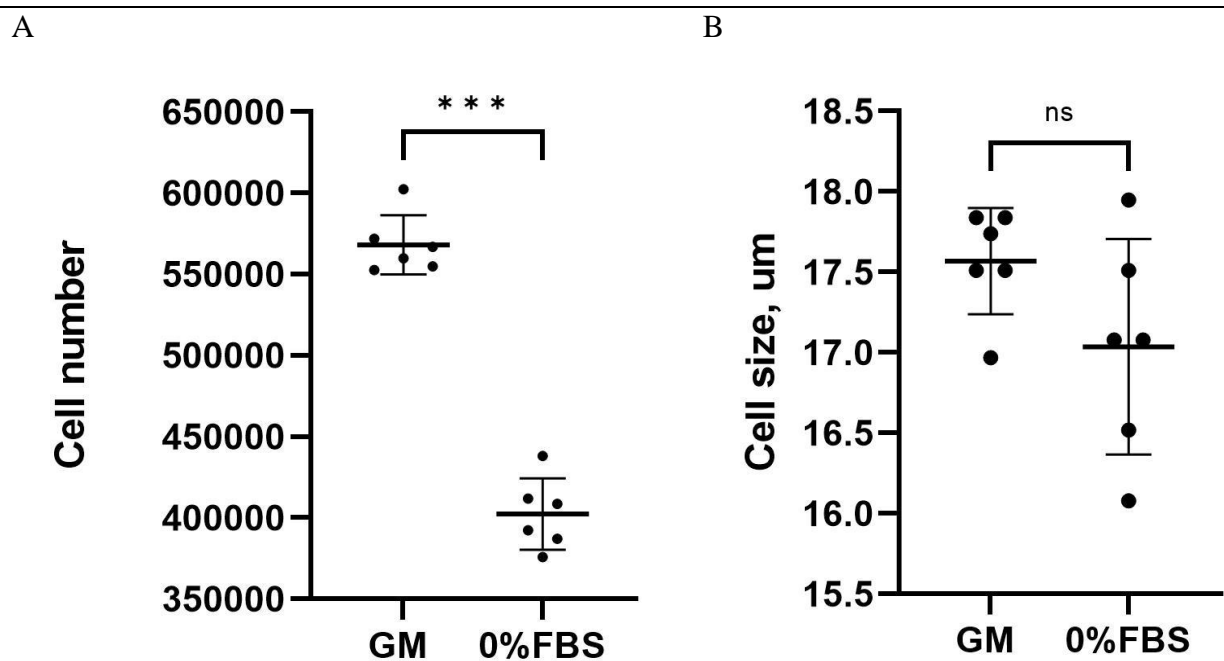
Target gene	Sequence name	Sequence (5' to 3')
ACAT2	Fw_hACAT2_248	CTCGGCTGCTGCGAGTTGTG
	Rv_hACAT2_491	GAGTAGGGAATTCCTGCACCCA
FASN	Fw_hFASN_987	ATACATCGAAGCCCACGGCA
	Rv_FASN_1209	GGGGCTATGGAAGTGCAGGT
18S rDNA	18S rDNA of nuclear DNA	TCGGAACTGAGGCCATGATTA
	18S rDNA of nuclear DNA rev	GCGGGTCATGGGAATAACG

Table S3. List of reagents

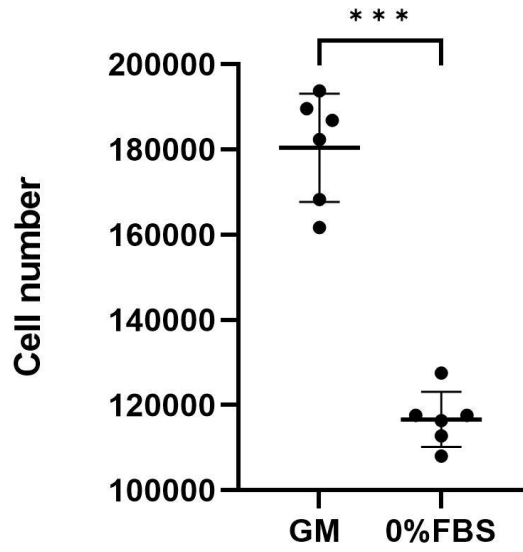
REAGENT or RESOURCE	SOURCE	IDENTIFIER
Dulbecco's modified Eagle's medium F-12 (DMEM/F-12)	US Biological life sciences	Cat#D9807
Fetal Bovine Serum (FBS)	Sigma-Aldrich	Cat#F7524
Streptomycin sulfate salt	Sigma-Aldrich	Cat#S9137-100G
Penicillin G sodium salt	Sigma-Aldrich	Cat#P3032
Trypsin	Biowest	Cat#X0930-100
TRIzol	Ambion by life technologies	15596018
L-glutamine	Sigma-Aldrich	Lot # SLBW9892
Nuclease-Free water	Invitrogen	AM9930
Qubit RNA HS Assay Kit	Invitrogen	Q32852
Illumina TruSeq Stranded Total RNA kit	Illumina	N/A
10x Standard <i>Taq</i> reaction buffer	New England Biolabs	B9004S, LOT # 410114545
dNTPs	New England Biolabs	N0447S, LOT # 10109034
<i>Taq</i> DNA polymerase	New England Biolabs	M0267S, LOT # 10052002
Ethidium Bromide Solution	Bio-Rad	1610433
Agarose	Fisher Scientific	BP1356-500, LOT # 117161
Sodium bicarbonate	Sigma-Aldrich	S57761-500G, LOT # SLBX3650
Poly(ethylene glycol)	Sigma-Aldrich	95172-250G-F, LOT # BCCF4379

Nonidet-P40 substitute	US Biological Life Sciences	N3500 LOT # L12120474
Glycerol	Sigma-Aldrich	G5516-500ML, LOT # SHBL3980
Sodium phosphate dibasic	Sigma-Aldrich	S0876-1KG, BCCF9941
Potassium phosphate monobasic	Sigma-Aldrich	P5379-1KG, BCCF3888
Magnesium chloride	Sigma-Aldrich	M8266-1KG, LOT # SLCJ1339
SYBR Green PCR Master Mix	Applied Biosystems	4309155, LOT # 2205536
1kb DNA Ladder	New England Biolabs	#N0552S
Gel loading dye	New England Biolabs	B7024A
TaqMan Reverse Transcription Reagents	Applied Biosystems	N80802234, LOT# 2373972

Figure S1. Dot plots for the HeLa cell line growth model under the FBS-deprived conditions point out cell number and cell size across the three time periods. (A) and (B) represents 24h, while (C), (D) represents 48h, (ns; not significant, **, P<0.01, ***, P<0.001, Unpaired t-test).



C



D

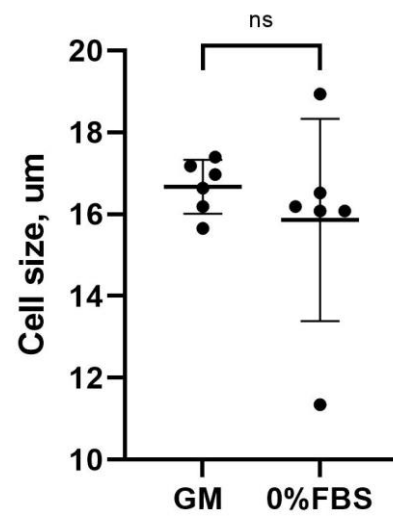


Figure S2. Dot plots for the A549 cell line growth model under the Complete medium (GM) and FBS-deprived (0%FBS) conditions point out cell size at 16hrs, (***, $P < 0.001$, Unpaired t-test).

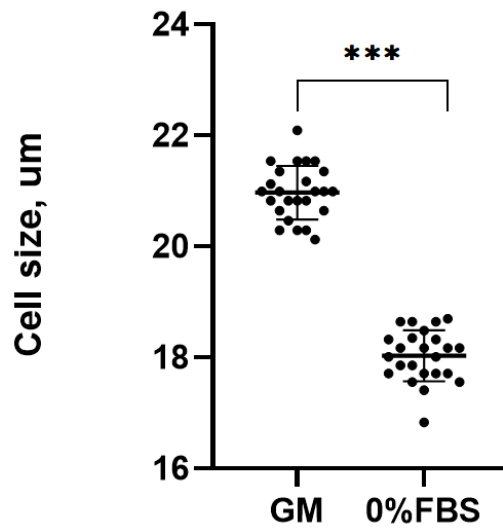


Figure S3. The ribosome/polysome profiling of A549 cancer cells incubated for 24h in media with glucose supplement represented by blue line or without glucose supplement represented by the black line in the graph.

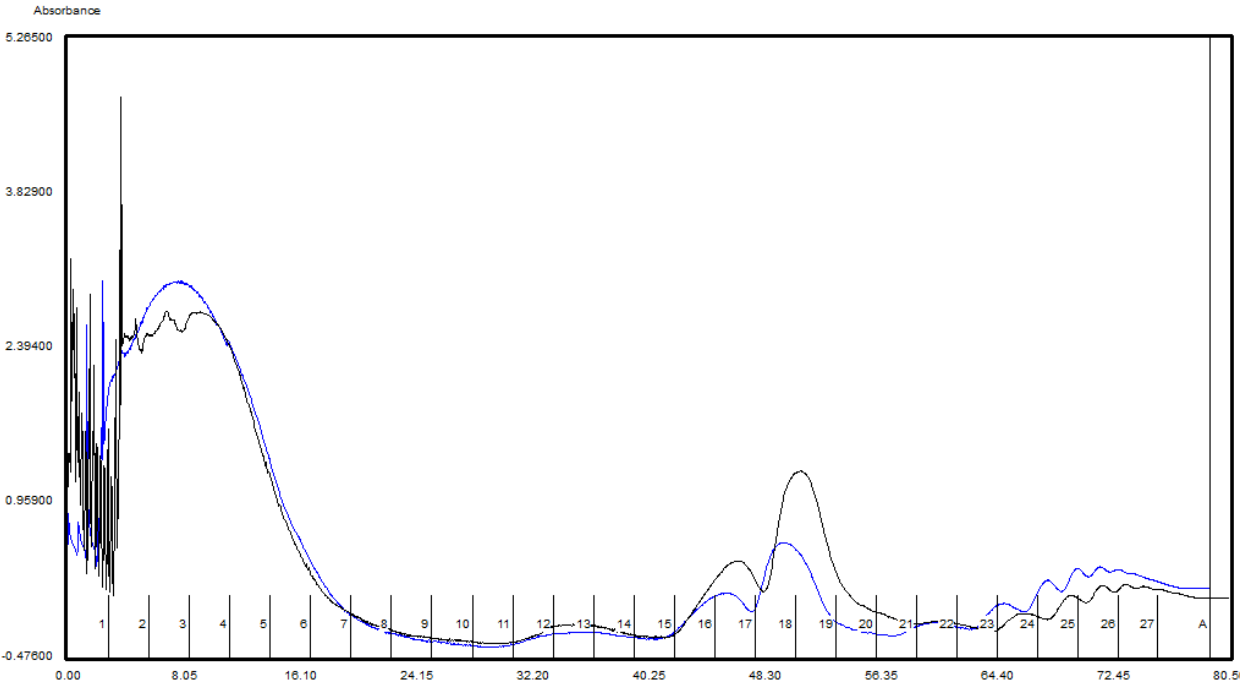


Figure S4. The ribosome/polysome profiling of A549 cancer cells incubated for 24h with serum with complete media represented by blue line or without amino acid supplement represented by the black line in the graph.

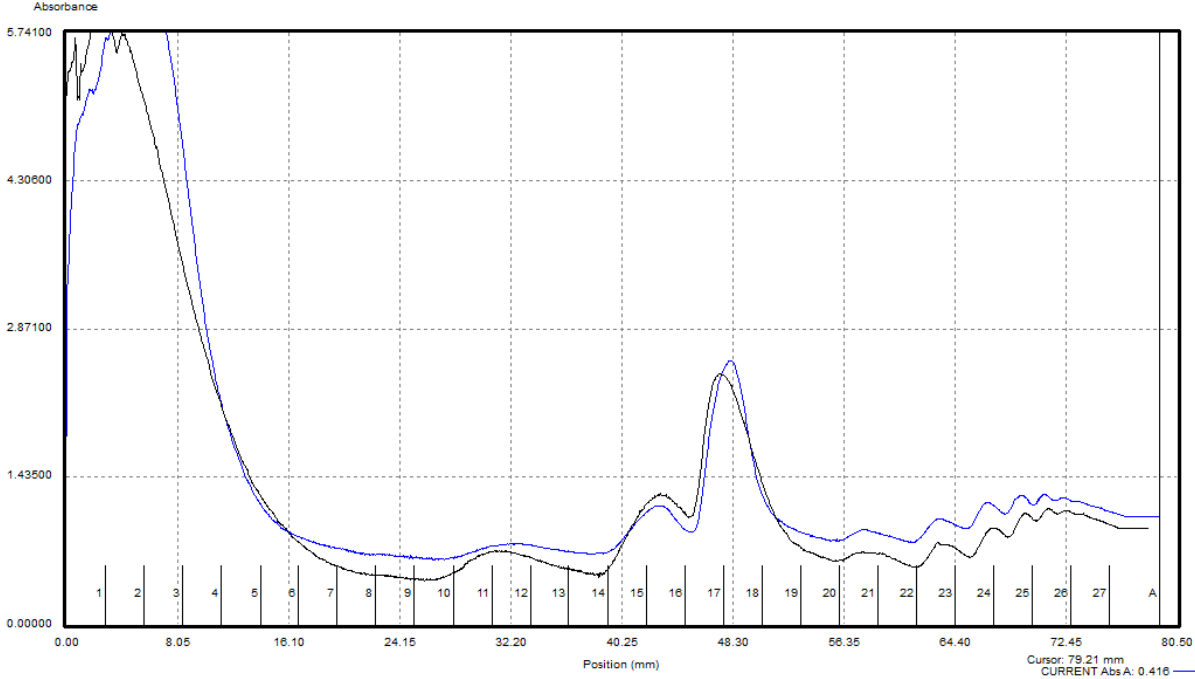


Figure S5. The ribosome/polysome profiling of HEK293 cancer cells incubated for 24h with serum (10% FBS) represented by black line or without serum represented by the blue line in the graph.

